

RESEARCH

Open Access



Optimizing Pozzolanic Concrete Mixtures Using Machine Learning and Global Sensitivity Analysis Techniques

Dina M. Abdelsattar¹, Mahmoud Owais^{1,2} , Mohamed F. M. Fahmy¹ , Rahma Osman¹ and Mohamed K. Nafadi^{1*}

Abstract

The cement industry is a significant contributor to CO₂ emissions worldwide, which demands new measures to reduce its environmental impacts. Therefore, finding solutions to reduce the CO₂ emissions in cement production became necessary. Pozzolanic materials offer an optimum solution approach with both environmental and functional advantages. For the investigation of pozzolan effects on the concrete mixture, the modeling part becomes a challenging task. This study models and predicts the compressive strength of pozzolanic cement-based concrete using deep residual neural networks (DRNNs) and variance-based sensitivity analysis (VBSA). The designed DRNNs architecture uses shortcuts (i.e., residual connections) that bypass some layers in the deep network structure in order to alleviate the problem of training with high accuracy. The research also examines crucial aspects such as pozzolan type, substitution ratio, component proportions, and grinding processes, using data developed by the authors and from different pozzolanic concrete compositions from various studies. The proposed model showed a high accuracy of $R^2 = 0.94$ for testing data that outperformed traditional literature models, enabling the generation of a large sample of synthetic experimental data for further analysis. The VBSA improves knowledge by prioritizing the importance of input factors, resulting in a complete method for designing concrete mixes. The analysis revealed that silica fume and volcanic ash were the most effective pozzolans in enhancing compressive strength, followed by scoria and metakaolin, with optimal substitution ratios ranging from 10 to 15% for most natural pozzolans and up to 20–30% for metakaolin and pumicite. Hence, this newly presented analysis framework offers an optimizing tool for pozzolanic concrete mix design that could investigate several pozzolana types/proportions, their efficiency, and the structural performance of the final concrete mixture.

Keywords Concrete mixtures, Deep learning, Global sensitivity analysis, Variance-based models, Pozzolanic cement, Sustainable concrete, Machine learning

1 Introduction

Cement production is a highly polluting industry that significantly harms the environment due to its substantial emissions. As a sizeable energy-consuming sector, the cement industry negatively impacts environmental sustainability, mainly by releasing organic pollutants (Jokar & Mokhtar, 2018). The process of cement production requires vast energy, from the diesel used to transport raw materials to the mills, to the fuel needed to operate the mills and heat the kilns. The heating of raw materials in kilns, essential for

Journal information: ISSN 1976-0485 / eISSN 2234-1315.

*Correspondence:

Mohamed K. Nafadi
mknafadi@aun.edu.eg

¹ Civil Engineering Department, Faculty of Engineering, Assiut University, Assiut, Egypt

² Sphinx University, New Assiut, Egypt



© The Author(s) 2025. **Open Access** This article is licensed under a Creative Commons Attribution 4.0 International License, which permits use, sharing, adaptation, distribution and reproduction in any medium or format, as long as you give appropriate credit to the original author(s) and the source, provide a link to the Creative Commons licence, and indicate if changes were made. The images or other third party material in this article are included in the article's Creative Commons licence, unless indicated otherwise in a credit line to the material. If material is not included in the article's Creative Commons licence and your intended use is not permitted by statutory regulation or exceeds the permitted use, you will need to obtain permission directly from the copyright holder. To view a copy of this licence, visit <http://creativecommons.org/licenses/by/4.0/>.

forming clinker—the primary component of ordinary Portland cement (OPC)—produces harmful emissions such as sulfur dioxide (SO_2), nitrogen dioxide (NO_2), and carbon dioxide (CO_2). The cement industry is estimated to be responsible for approximately 8% of greenhouse gas emissions (Belaïd, 2022), making it a significant contributor to global warming. Moreover, dust emissions are released during the limestone crushing, clinker production, cement manufacturing, and packing stages, further contributing to environmental degradation (Katare & Madurwar, 2020).

In Egypt, for instance, the cement industry has grown greatly in size and capacity over the last 30 years. In 1975, four factories produced 4 million tons per year. Until 2016, 14 factories produced nearly 38 million tons of clinker per year, primarily from dry kilns, with only a tiny amount from seven wet kilns in two companies. Egypt's production is estimated to be 1.5% of world production. According to Ali et al. (2016), the manufacturing consumption of raw materials (estimated as tons per year) is shown in Fig. 1. Consequently, the pollutants emitted by cement plants became further concerning. For example, some plants release as much as $23,648 \text{ Mg/m}^3$ of dust into the atmosphere, along with 512.48 Mg/m^3 of carbon monoxide (CO), 25.27 Mg/m^3 of sulfur dioxide (SO_2), and 130.69 Mg/m^3 of nitrogen dioxide (NO_2). These emissions contribute significantly to air pollution and exacerbate health risks for nearby populations while also playing a role in climate change. The high emissions levels, especially dust and CO_2 , emphasize the urgent need for cleaner and more sustainable production methods. Addressing these environmental challenges is critical to reducing the industry's carbon footprint and protecting the environment and public health (Ali et al., 2016).

Different suggested/applied approaches reduce CO_2 emissions as much as possible. There are different options to reduce the required energy and greenhouse gas emissions from the cement industry; one of them

is to change the manufacturing system/criteria (e.g., applying CO_2 storage and capture technique). Another one is to replace partially/fully the clinker/cement with pozzolanic materials. The pozzolanic cement (PzC) is produced either by partially replacing the clinker or partially replacing the cement in the concrete mixture (blended cement). The PzC industry not only contributes to reducing CO_2 emissions, but also helps to use existing natural resources and save disposal costs of byproducts waste. One more eco-friendly property of PzC is that it can react with Ca(OH)_2 with reduced heat emissions, unlike the OPC. Therefore, using PzC helps to minimize the energy required to produce cement and the heat of hydration to produce cement composite (Altawir & Kabir, 2010; Dunuwela & Rajapakse, 2018).

The energy consumption in cement production mainly results from the grinding and clinkering processes. Using pozzolans to replace the clinker/cement can reduce energy consumption in grinding (depending on the grain size) and thermal energy required for clinkering, because they would be used as they are. Reference (Ghiasvand et al., 2014) found that grinding the pozzolana (Trass) as a replacement for clinker required less energy than grinding it as a cement replacement in concrete to achieve the same percentage of $45 \mu\text{m}$ residue. Furthermore, reference (Rashwan et al., 2023a) found that replacing cement with 10% by weight of Pozzolana (mafic rocks) resulted in a 13.75% decrease in energy consumption to produce 1 ton of binder. Reducing the burning process rate of raw materials will help reduce pollutant emissions. Using the PzC seems to be a promising solution to reduce the rate of carrying out that process, which is assumed to be the leading cause of CO_2 emissions.

The incorporation of pozzolana in the cement and concrete industry is influenced by several key factors that dictate the behavior and performance of the resulting concrete. Some of these factors are directly related to the pozzolana itself, including the type of pozzolan used, its chemical composition, fineness, the proportion incorporated in the mixture, the stage at which it is introduced (whether during clinker production or directly into the cement), and the number of pozzolan types included in the mix. Additionally, factors related to the other components of the concrete mixture play a significant role. As a result, optimizing pozzolanic concrete mixtures requires careful consideration of all these variables to produce a more sustainable and efficient green concrete (Chihaoui et al., 2022; Golewski, 2022).

Recent studies have been concerned with developing models that help predict concrete behavior based on experimental data from previous studies (Haq et al., 2024; Karim et al., 2024; Mottakin et al., 2024; Owais &

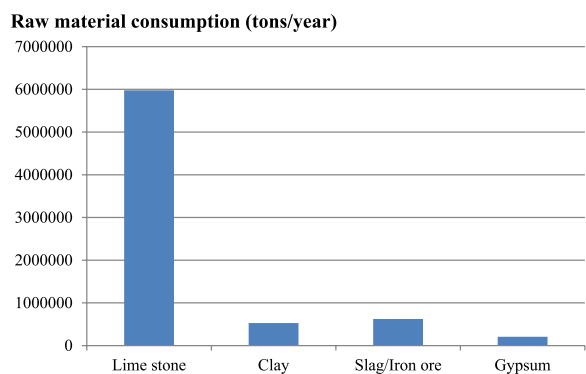


Fig. 1 Manufacturing consumption of raw materials from an Egyptian cement plant (Ali et al., 2016)

Idriss, 2024). Modeling data play a crucial role in saving time and resources in labs by providing predictions that closely approximate experimental outcomes. Despite this, relatively few studies have focused on developing models specifically for optimizing pozzolanic concrete mixtures. This study bridges the gap by introducing a novel machine learning (ML) framework, specifically a deep residual neural network (DRNN), combined with variance-based sensitivity analysis (VBSA)—an innovative global sensitivity analysis (GSA) tool. This approach aims to accurately identify and prioritize the factors influencing the behavior of pozzolanic concrete.

The DRNNs architecture is particularly well-suited for this purpose because it can handle complicated, non-linear interactions between controlling variables, allowing for more exact predictions of concrete performance under different situations (Alshehri et al., 2023; Owais, 2024a). The VBSA, which uses the DRNN model, offers a systematic technique for determining the relative importance of each parameter (Owais & Moussa, 2024). This method emphasizes the most critical aspects that affect pozzolanic concrete behavior, such as pozzolan type, composition, and mix proportions, as well as how these parameters interact with other components in the mixture. The newly provided analytical methodology, which integrates DRNNs and VBSA, has the potential to considerably increase our knowledge of pozzolanic concrete mixes. It provides a useful tool for creating optimum mixes adapted to particular applications, resulting in more efficient, durable, and sustainable concrete solutions.

The rest of the article is organized as follows: The next section reviews the current state of research on related topics to emphasize this article's contribution. Section 3 describes the input data and the relevant factors under investigation. Section 4 outlines the analytical framework along with the associated mathematical and statistical methods. Section 5 discusses the modeling outcomes and sensitivity analysis results. The final section provides the research conclusions.

2 State of the Art

This section is divided into five subsections. The first subsection characterizes the different types of pozzolana and their manufacturing procedures. The second subsection reviews the advances in the pozzolanic industry and the various contributions of previous studies in enhancing concrete mixture properties through pozzolana. The third subsection explores the application of ML tools, particularly the DRNNs, for predicting the mechanical properties of pozzolanic concrete mixes. The fourth subsection delves into the use of the GSA in modeling, explaining its relevance

in evaluating the influence of various parameters on concrete performance. Finally, the fifth subsection highlights the unique contributions of this study, including its novel approach and significant findings concerning the optimization of PzC concrete mixtures.

2.1 Advances in the Pozzolanic Industry

Pozzolana is a non-cementitious material primarily composed of silica or a combination of silica and alumina. While it is not inherently cementitious, pozzolana reacts with the calcium hydroxide (Ca(OH)_2) produced during the hydration of cement, forming additional calcium silicate hydrate (C-S-H), which enhances the strength and durability of the concrete (Hamada et al., 2023). There are two main types of pozzolana: natural pozzolana (NPz) and artificial pozzolana (APz). NPz are derived from geological sources, while artificial pozzolans are typically industrial or agricultural byproducts. NPz can be further classified into two groups based on their origin: sedimentary and volcanic. Sedimentary natural pozzolans include diatomaceous earth, naturally calcined clay, opaline silica, and cherts (Chindaprasirt & Rukzon, 2008). Volcanic pozzolans include volcanic ash, tuffs, pumice, and slag. NPz can be used in their natural state or undergo mechanical or thermal processing to improve their reactivity and efficiency (Waghmare et al., 2021). APz, on the other hand, are sourced from waste products generated by industries or agriculture. Examples include fly ash, rice husk ash, blast furnace slag, silica fume, palm oil fuel ash, marble dust, sugarcane bagasse ash, and synthetic zeolites. Both NPz and APz contribute to the pozzolanic reaction by reacting with Ca(OH)_2 during cement hydration, forming more C-S-H while minimizing the generation of excess heat (Papadakis, 2000). This results in improved long-term performance of concrete, particularly in terms of strength and durability. Figure 2 illustrates the primary types of pozzolans.

Using NPz offers sustainable and eco-friendly benefits to cement production by partially substituting clinker with natural resources, thus reducing the environmental impact of cement manufacturing. The natural characteristics of some NPz make them suitable as clinker substitutes, especially since they undergo similar processes, such as quenching, which is the rapid cooling of volcanic materials. This substitution reduces the reliance on clinker, leading to lower carbon emissions and a more sustainable cement product. However, one of the challenges associated with NPz is its tendency to reduce early strength in concrete. This drawback may be attributed to the larger particle size of NPz grains, which slows down the initial hydration process. Nevertheless, this issue can be mitigated by grinding the NPz to the nanoscale, which enhances its

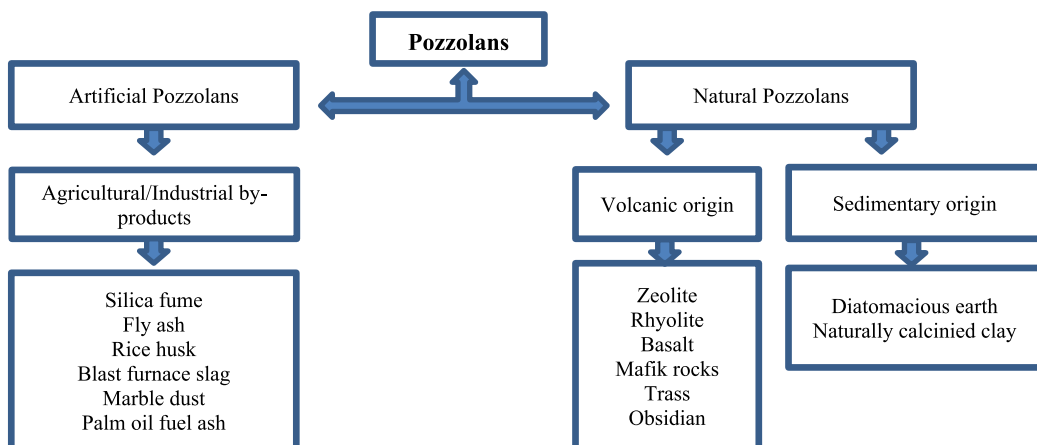


Fig. 2 The main classification of pozzolana

reactivity and compensates for the early strength loss (El-Didamony et al., 2015). Most of the natural pozzolans studied are volcanic tuffs, with the most common types including basalt, rhyolite, trachyte, zeolite, pumice, trass, and obsidian. The natural formation of NPz generally eliminates the need for additional thermal processing, saving energy that would otherwise be required. Due to its availability as a natural resource, NPz is also cost-efficient. Studies have shown that incorporating NPz into cement significantly reduces the heat of hydration. Furthermore, NPz contributes to long-term hydration, resulting in improved workability and, over time, higher compressive strength. NPz also enhances the durability of concrete by increasing resistance to sulfates and chlorides. The performance of NPz in cement is influenced by several factors, including particle size distribution, specific surface area, chemical composition, and crystallinity (Záleská et al., 2018).

On the other hand, APz contributes to sustainability by utilizing industrial and agricultural byproducts, such as fly ash, rice husk ash, and silica fume. The APz, derived from industrial waste, offers environmental

benefits by reducing disposal costs and preventing pollution from open waste dumps. The high specific surface area and fineness of most APz types accelerate the hydration process, which leads to early strength gain but can reduce workability and emit higher heat of hydration. According to previous studies, APz can replace clinker or cement in higher proportions than NPz, making it a highly effective substitute (McCarthy & Dyer, 2019; Nourredine et al., 2021; Ramezanianpour, 2014). Several factors affect the efficiency of both natural and artificial pozzolans in cement mixtures (Joshua et al., 2018). Table 1 summarizes the key factors influencing pozzolans' performance, highlighting their advantages and limitations.

The efficiency of pozzolans is primarily evaluated based on their chemical, physical, and mechanical properties. Their pozzolanic activity is determined by how well they meet the characteristics specified in various standards. Pozzolans can be incorporated into the cement production process in two ways: by partially replacing clinker during cement manufacturing or by substituting cement directly in concrete mixtures. Both methods are

Table 1 Factors affecting the efficiency of pozzolana.

Efficiency terms	Natural pozzolans	Artificial pozzolans
With	<ul style="list-style-type: none"> - Natural resource ✓ Can be used without thermal processing to substitute clinker ✓ Save energy and cost-efficient ✓ Low heat of hydration ✓ High workability ✓ Higher compressive strength in later ages ✓ Ecofriendly ✓ Durable product 	<ul style="list-style-type: none"> Save waste disposal cost of the byproducts Ecofriendly High early strength Higher possible Substitution ratio than the NP
Against	<ul style="list-style-type: none"> ✗ Low early strength ✗ Pozzolanic characteristics differ for the same type of NP according to location, age of the rock 	<ul style="list-style-type: none"> Lower workability Higher heat of hydration Energy consuming

environmentally sustainable. However, replacing clinker with pozzolan during cement production is generally more cost-effective and energy-efficient (Nayaka et al., 2018).

To assess the quality and effectiveness of pozzolana—whether natural or artificial—various physical, chemical, and mechanical tests must be conducted. Reference (Záleská et al., 2018) suggested three sets of characterization methods. The first set focuses on fundamental physical and chemical prerequisites for a material to qualify as pozzolan suitable for blended cement, such as granulometric tests, oxide analysis, and molecular spectroscopy. The second set examines the reactivity of the pozzolan through tests like quantitative X-ray diffraction (XRD), pozzolanic activity evaluation, and scanning electron microscopy (SEM) combined with energy dispersive spectroscopy (EDS). The third set evaluates the mechanical properties. Table 2 summarizes the characterization methods outlined in previous studies.

Several key characteristics, including particle size distribution, specific surface area, chemical composition, and crystallinity, influence pozzolana's performance in cementitious materials. According to previous studies, the properties of the pozzolan used—such as boiler ash—are highly dependent on factors like the source of the material, industrial combustion processes, collection methods, cooling techniques, particle size, and phase state (Katare & Madurwar, 2020). These factors play a critical role in determining the overall quality and reactivity of the pozzolan. The oxide composition of pozzolana, particularly its silica (SiO_2) content, is a fundamental parameter in evaluating its suitability for use in concrete. As highlighted in previous research, the predominant component of pozzolana is SiO_2 . Various

standards dictate that the combined content of SiO_2 , Al_2O_3 , and Fe_2O_3 should exceed 70% to ensure adequate pozzolanic activity. Reference Hamada et al., (2023) reviewed previous studies and found that the contents of SiO_2 , Al_2O_3 , and Fe_2O_3 existed in NPz were (40–80)%, (10–20)%, and (0–13)%, respectively.

Characterizing pozzolana is essential for predicting the performance of the resulting cementitious composites. It enables the determination of optimal dosages in concrete mixtures, which is crucial for designing sustainable and efficient concrete with reduced environmental pollutants. By understanding the physical and chemical properties of pozzolana, engineers can optimize concrete formulations to achieve the desired mechanical properties and long-term durability (Hung et al., 2018).

2.2 Pozzolanic Cement in Concrete Mixtures

Incorporating PzC significantly influences cementitious composites' properties in both their fresh and hardened states. Various studies have examined the effects of adding pozzolanic materials to cement matrices, focusing on factors like density, water demand, heat of hydration, setting times, and workability for fresh concrete, as well as compressive, flexural, and splitting strengths, permeability, and durability for hardened concrete. The performance of PzC concrete is influenced by several key factors, including the type of pozzolana used, pozzolan-to-clinker/cement ratio, chemical composition, the number of pozzolanic materials involved, and the fineness of the pozzolan (Dembovska et al., 2017; Senhadji et al., 2012).

The workability of PzC concrete can be measured using slump tests for normal concrete and flow tests, L-box, and V-funnel tests for self-compacting mortar (Hamada et al., 2023). Initial and final setting times are also key indicators

Table 2 Pozzolan characterization methods.

Characterization	Methodology	Estimation	Limits/ASTM
Granulometry		Laser diffraction	Particle size upper limit (45 μm)—40% residue
Oxides/elemental analysis		X-ray fluorescence	$\text{SiO}_2 + \text{Al}_2\text{O}_3 + \text{Fe}_2\text{O}_3 > 70\%$
Molecular spectroscopy		Detect harmful organic substances if exist	—
Reactivity tests	Frattini test	Qualitative (pozzolanic/not)	—
	Chapelle test	Quantitative giving the amount of portlandite in mg fixed by 1 g of the material	The lower limit of 650 mg portlandite/g of material
Compressive strength of pastes	Strength activity index SAI	Qualitative	SAI $\geq 75\%$ for 28-days cured samples
	Pozzolan effectiveness coefficient PEC	Quantitative	<ul style="list-style-type: none"> • $0 < \text{PEC} < 1$ then acts as pozzolan • $\text{PEC} < 0$, then acts as filler only • $\text{PEC} > 1$ PzC then better than the OPC

of workability. For instance, reference Hassan et al., (2019) replaced cement clinker with synthetic zeolite at ratios of 1, 3, 5, 7, and 10%, increasing the setting time and thereby improving workability. Another study found that replacing 25% of cement with volcanic tuffs (rhyolite) resulted in initial and final setting times ranging from 160 to 215 min and 200 to 255 min, respectively (Eldahroty et al., 2023). The fineness and content of pozzolans also impact workability. Finer particles tend to fill voids more efficiently, thereby improving workability (Zeyad & Almaliki, 2021). However, increasing the volcanic ash content can reduce workability (Hammat et al., 2021). The reactivity of certain pozzolans, such as volcanic ash, zeolites, and diatomaceous earth, tends to improve over time (Abrão et al., 2020). Mixing water demand increases when clinker is replaced with NP due to particle agglomeration, high specific surface area, and internal porosity (Juenger & Sidique, 2015).

The density of PzC concrete is another important factor. A study in Omrane and Rabehi (2020) found that replacing cement with natural pozzolana (NP) in recycled self-compacting concrete (SCC) reduced the density by 0.88, 1.46, 1.72, and 1.94% for replacement ratios of 5, 10, 15, and 20%, respectively, due to the lower density of NPz compared to cement.

Regarding heat of hydration, PzC is expected to reduce the overall heat release. For example, reference Al-Chaar (2013) replaced cement with three different NPz and compared between the results of the heat of hydration test of

one of them from Saudi Arabia (Pozzolan S1), and class F Fly ash. The results showed that the heat of hydration of S1 was less than the one of the FA mixture by 15%, while the FA mixture resulted in less heat of hydration than the control mixture by 30%. Another study in Eldahroty et al. (2023) showed that replacing 25% of cement with volcanic tuffs reduced the heat of hydration from 303.9 J/g in the reference sample to between 269.9 and 289.6 J/g after 7 days.

The compressive strength of concrete is often the most important characteristic affected by incorporating pozzolanic cement into a cementitious matrix. Several studies have explored the effects of using both NPz and APz types as partial replacements for clinker or cement on the compressive strength of resulting concrete. Some studies have even examined the simultaneous use of multiple types of pozzolana. Reference Dwivedi et al., (2006) investigated bamboo leaf ash as a substitute for 20% of the cement, finding that it exhibited comparable compressive strength at 28 days to control samples, with pozzolanic reactivity increasing over time and at higher temperatures. In another study, fresh basalt powder was used to replace up to 20% of ordinary cement paste, resulting in improved mechanical properties (El-Didamony et al., 2015). Figure 3 depicts the compressive strength of concrete over time with different portions of basalt (Moawad et al., 2021). Similarly, reference (Moawad et al., 2023) studied the behavior of high-strength concrete (HSC) with 5, 10, and 15% natural basalt, concluding that 10% replacement

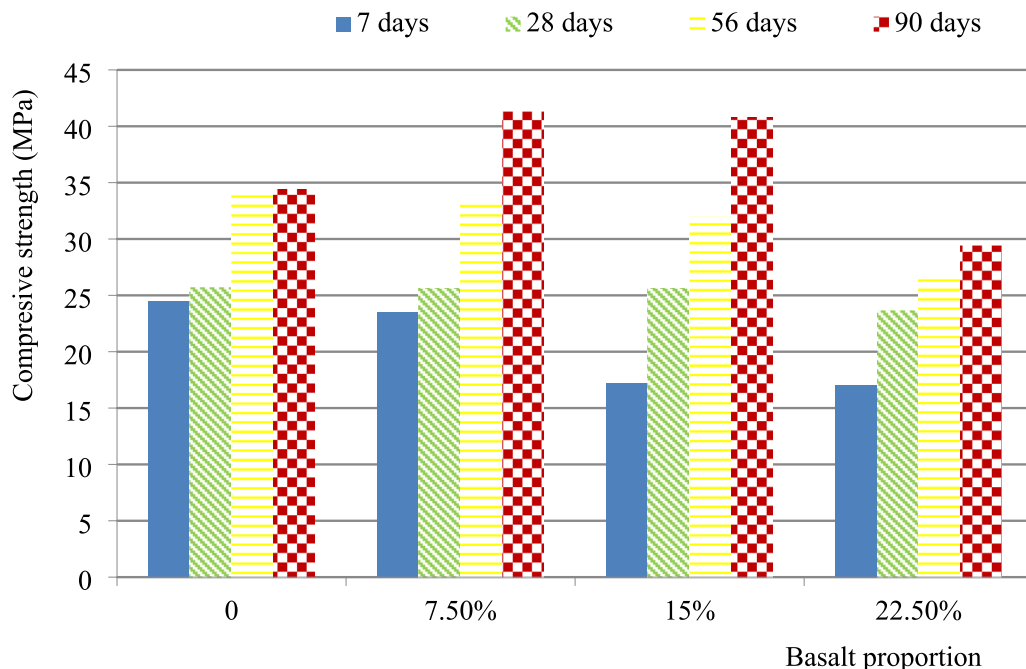


Fig. 3 Compressive strength of concrete after 7, 28, 56, and 90 days using 7.5%, 15%, and 22.5% of basalt.

was the optimal ratio. Reference Moawad et al., (2023) also examined using 25% basalt to replace the clinker, and found that this proportion yielded good results in terms of compressive strength and pozzolanic reactivity.

Studies also explored using volcanic ash or volcanic tuff as clinker or cement replacements. For example, reference Ghiasvand et al., (2014) used Trass as a clinker and cement replacement at 25 and 35%, both in fine and coarse states. The compressive strength values after 7, 28, and 90 days were higher for fine Trass, especially at 28 and 90 days, as shown in Fig. 4. The results indicated that finer pozzolana particles produced stronger concrete, and replacing clinker with pozzolana consumed less energy than replacing cement. Table 3 shows the differences in the compressive strength values between the replaced clinker and the replaced cement by the same proportion of 25% of Trass (fine).

In the same study, the same proportions were used as cement replacement in concrete mixtures, and the samples were tested under compression to compare the results (Ghiasvand et al., 2014). The compressive strengths of the concrete mixtures with Trass replacing cement are shown in Fig. 5. When the cement was partially replaced by Trass, the compressive strength of the fine cement mixtures was still higher than in other cases. However, at a 25% replacement level, the compressive strength was lower compared to non-replaced fine cement. This contrasts clinker replacement, which resulted in higher compressive strength at the same proportion. Further findings of Rashwan et al., 2023b suggested that using ophiolitic mafic

Table 3 Compressive strength values of the OPC replaced clinker and replaced cement by 25% of Trass after 7, 28, and 90 days.

25% substitution for	Compressive strength (MPa)		
	7d	28d	90d
OPC (fine)	33	42	46
Clinker (fine)	27	43	47
Cement (fine)	25	41	43

rocks (OMR) in cement paste at 5% or 10% replacement levels increased compressive strength at all curing stages.

The authors of the present research recently contributed to an experimental study on pozzolanic concrete's strength development (Hassanein et al., 2022). The study used six different types of cement: ordinary Portland cement CEM I-42.5N, sulfate resisting cement CEM I-42.5-SR-5; two types of Portland pozzolanic cement with different grades CEM II/B-P(42.5) and CEM II/B-P(32.5), sulfate resisting pozzolanic cement CEM IV/A(P) 42.5SR, and low heat Portland pozzolanic cement CEM II/B-P (32.5N) L.H. The study included casting concrete mixtures with a design compressive strength of 25 MPa. The samples were tested at different ages, ranging from 3 to 180 days. Selected measured compressive strengths of the tested concrete samples are shown in Fig. 6. All concrete mixtures achieved the required strength for all investigated cement types. Regarding strength development, all concrete mixtures

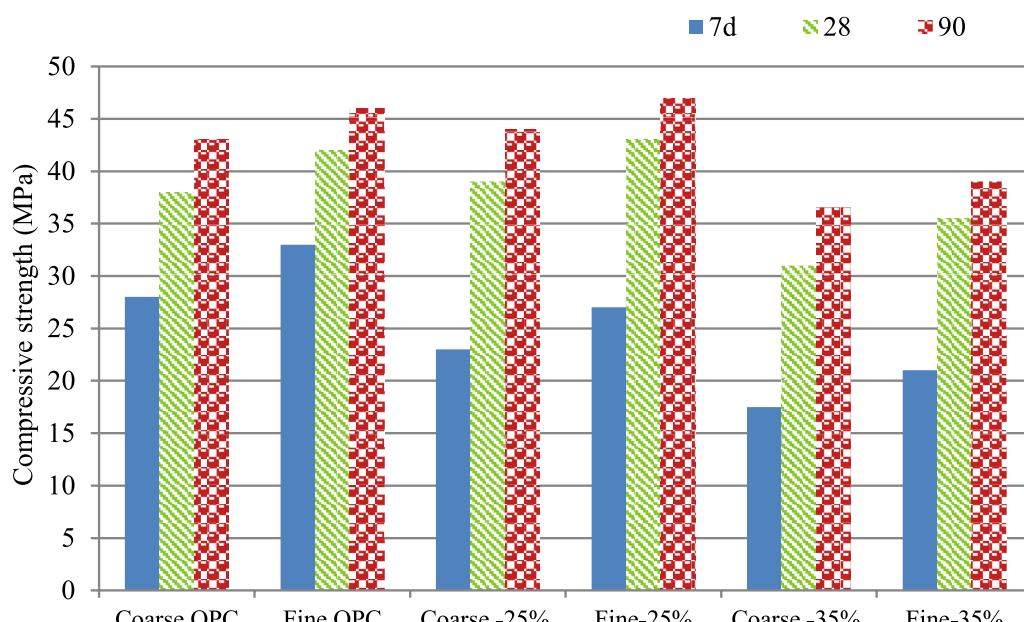


Fig. 4 Compressive strengths of concrete mixes made up of cement containing different proportions of Trass as a clinker replacement.

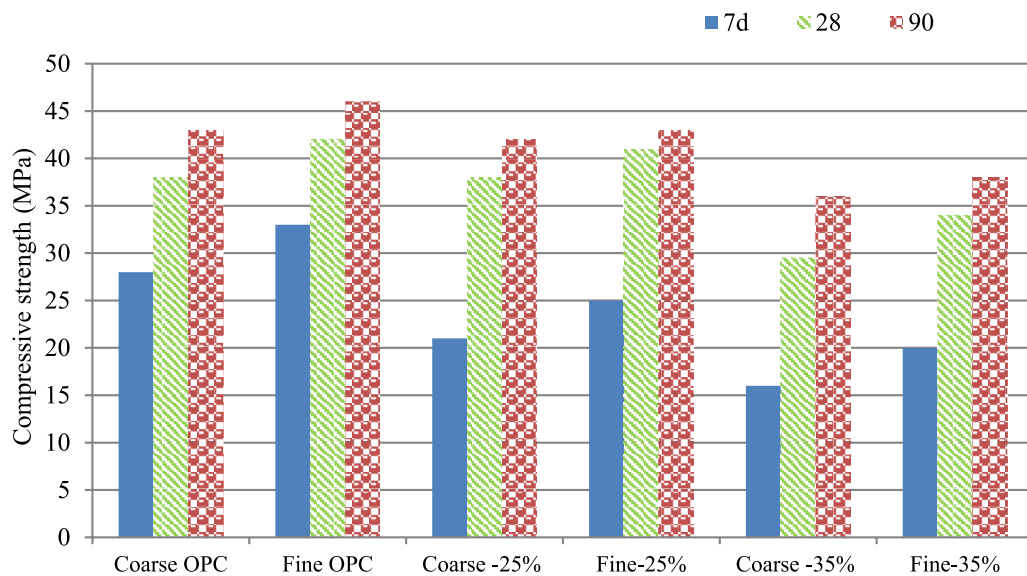


Fig. 5 Compressive strengths of concrete mixes made up of cement containing different proportions of Trass as a cement replacement.

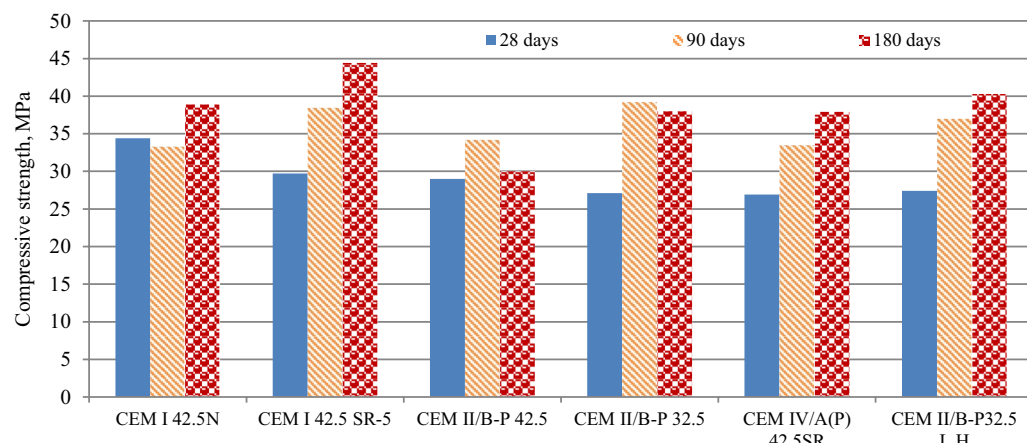


Fig. 6 Compressive strengths of concrete mixtures using six types of cement at 28, 90, and 180 days.

showed an increase or stabilization with the concrete age, except for CEM II/B-P(42.5), which showed slightly lower strength at 180 days than that for 90 days. The study recommended further research on the strength development of high-strength pozzolanic concretes and investigating the potential effects of different admixture types on their performance over time.

In conclusion, the above studies contribute valuable insights to optimizing pozzolanic cement mixtures. This database of findings can inform the development of advanced models, such as DRNNs, to predict the performance of PzC concrete mixture, thereby supporting sustainability and enhancing concrete efficiency.

2.3 Modeling Attempts of Pozzolanic Concrete Mixture

Numerous efforts have been made to optimize pozzolanic concrete mixtures using advanced computational techniques. These approaches aim to improve the accuracy and efficiency of predicting critical properties such as compressive strength, workability, and durability by utilizing various artificial intelligence (AI) and machine learning models.

Predicting the compressive strength of pozzolanic concrete using natural pozzolans was first attempted in reference Rebouh et al., (2017) by combining neural networks (NNs) with genetic algorithms (GAs). Their hybrid NN-GA model showed strong predictive power with a high correlation value of 0.93. By integrating the optimization capabilities of GAs with the prediction

capabilities of NNs, this approach advances state-of-the-art artificial intelligence model accuracy in the building materials domain.

Similarly, a computer-aided method for predicting pozzolanic concrete mixtures' slump and compressive strength was established in Kao et al. (2018). Their model—verified using experimental data—proved to be very beneficial for pozzolanic concrete mix design by allowing for more exact control over concrete qualities during the design phase. The technique considers the two most important aspects of concrete performance—its strength and workability.

To go even further, reference Moradi et al., (2021) examined the compressive strength of pozzolanic concrete with metakaolin (MK) or silica fume (SF) and compared two models, multiple linear regression (MLR) and artificial neural networks (ANN). According to their findings, the ANN model outperformed the MLR model significantly, with a correlation value of 0.9961. The study findings suggested that predicting the behavior of pozzolanic concrete using ANN models is the best option since they are better at capturing complicated non-linear correlations in material parameters.

In order to make these models even better, reference Ashrafiyan et al., (2024a) combined ANN with global sensitivity analysis to determine which variables most impact metakaolin concrete's compressive strength. They found that compressive strength was most affected by MK-specific surface area and $\text{SiO}_2/\text{Al}_2\text{O}_5$ ratio. Once they identified these critical factors, they helped create more efficient concrete mixes by increasing the model's predicted accuracies.

Using a REPtree model, pozzolanic concrete that incorporates industrial byproducts was evaluated more recently in reference (Ashrafiyan et al., 2024b). With a correlation value of 0.960 and an RMSE of 7.884 MPa, the REPtree model achieved better performance than other machine learning models, according to their analysis. A water-to-cement (w/c) ratio of 0.17, a superplasticizer-to-cement ratio of 1.88%, and a supplemental cementitious material-to-binder ratio of 0.15 were the ideal mix proportions predicted by this ensemble meta-model, which was created to forecast the cement content at 584 kg/m³. Utilizing industrial byproducts in their study highlights the possibility of implementing sustainable techniques in the manufacturing of concrete.

Other computational approaches have been investigated to further investigate the feasibility of using deep learning models and support vector machines (SVMs) for pozzolanic mixture performance prediction. These models, in conjunction with experimental solid databases, help researchers and engineers develop the ideal mix proportions that reduce material costs and

improve concrete manufacturing sustainability (Salami et al., 2021).

AI-based methodologies such as ANN, SVM, REPtree, and hybrid models like NN-GA may optimize concrete qualities in the design of pozzolanic concrete mixtures. These models can improve pozzolanic concrete's performance and longevity, facilitate the efficient investigation of mix design factors, and increase the precision of strength forecasts.

Despite these advances, the potential for applying DRNNs to predict the properties of PzC concrete remains an untapped opportunity. DRNNs, which have shown great success in handling complex, high-dimensional data in other applications (Alshehri et al., 2023; Idriss & Owais, 2024), could be particularly effective when paired with the GSA to better understand the underlying factors influencing pozzolanic concrete properties. Given that DRNNs have not yet been applied to this problem, it presents an exciting and valuable avenue for this study to be explored.

2.4 Global Sensitivity Analysis

Sensitivity analysis (SA) is typically performed as a post-processing step after the measurement or prediction of a variable. Due to the increasing demand for samples, conducting SA in laboratory conditions is often challenging, and thus, the majority of SA for material properties is carried out during the modeling phase. The accuracy of any SA technique heavily depends on the model's ability to simulate the effect of input factors on the output variable. In general, SA aims to assess how changes in the input variables of a numerical model affect the variations in the response (output) variable. The complexity and objectives of SA are determined by the specific modeling domain in which it is applied. Throughout the SA process, several critical decisions must be made by the analyst, starting with the selection of the output modeling approach, determining the input factor domain limits, deciding how to navigate the input factor space, and choosing the appropriate SA methodology (Owais et al., 2024).

SA is generally divided into two categories: local sensitivity analysis (LSA) and global sensitivity analysis (GSA), based on the extent of input factor variation. LSA focuses on measuring the sensitivity of the output factor by varying one input factor at a time, starting from a reference or ideal value, while keeping all other inputs at their nominal levels (e.g., the mean). In contrast, GSA takes into consideration changes in all input factors when evaluating sensitivity throughout the whole input factor space. Because of this, GSA is able to take into account interactions between input variables, while LSA is limited to analyzing "one-variable-at-a-time" (OAT). For a more

complete picture of input–output correlations, GSA may investigate both OAT and “all-variables-at-a-time” (AAT) (Schwartz et al., 2013).

To provide a more comprehensive view of the system’s behavior, GSA may also deal with cases where the input elements are constant or changing. Using the right approach to answer the questions posed is essential when doing SA. Some older methods are still in use, such as partial derivatives, but newer ones provide more sophisticated approaches, such as the elementary effects test (Morris, 1991), variance-based sensitivity analysis (Saltelli, et al., 2008), and density sensitivity (Spear & Hornberger, 1980). These approaches use various indicators, such as the variance of the distributions of the input variables or the correlation between them. However, most of these indicators, with the exception of partial derivatives, cannot be easily estimated analytically (Owais & Ahmed, 2022; Pianosi et al., 2016). Therefore, sampling algorithms, such as Latin Hypercube Sampling (LHS) or Monte Carlo (MC) simulations, are commonly employed to compute these indices (Tarantola et al., 2012).

Currently, GSA is widely used in a variety of applications, including model verification and calibration, uncertainty reduction, robust decision-making, and system controller analysis (Nguyen & Kok, 2007; Nossent et al., 2011; Shin et al., 2013; Sieber & Uhlenbrook, 2005). This is largely because GSA overcomes the limitations of LSA by providing a more holistic understanding of how input factors affect system performance. However, to the best of the authors’ knowledge, GSA has not yet been applied in the analysis of pozzolanic concrete mixtures. Therefore, one of the key contributions of this study will be the application of VBSA to PzC concrete mix design. This will provide a novel insight into the sensitivity of PzC properties to different input variables, allowing for more precise and reliable optimization of the mixture. By incorporating VBSA into the study of PzC mixtures, the research aims to improve our understanding of how various factors influence the performance of pozzolanic concrete and enhance the overall efficiency and sustainability of concrete mix design.

2.5 Research Significance

To this end, this study evaluates various types of pozzolana, assessing their effectiveness and optimizing their portions to create efficient, sustainable, and eco-friendly concrete. Additionally, it examines the best stage for incorporating pozzolana with cement by evaluating the recommended incorporation methods. To predict the compressive strength of pozzolanic concrete containing one or more natural or artificial pozzolanas, this study employs a novel framework of analysis based

on the DRNNs as an innovative ML tool and VBSA as one of the GSA techniques. The DRNNs demonstrated superior performance compared to traditional ML tools identified in the literature, significantly excelling in various accuracy metrics. Following the modeling phase, the VBSA is conducted to identify the primary factors influencing compressive strength. The main contributions of the current study can be summarized as follows.

2.5.1 First Application of DRNNs in Pozzolanic Concrete Modeling

To the best of the authors’ knowledge, this is the first study to apply Deep Residual Neural Networks (DRNNs) for predicting the compressive strength of pozzolanic cement-based concrete mixtures. While conventional neural networks (e.g., ANN, CNN, LSTM) have been applied in civil engineering contexts, the use of DRNNs—capable of deeper architectures without performance degradation—has not yet been explored in this domain.

2.5.2 Integration with Global Sensitivity Analysis (VBSA)

Although previous research has used basic sensitivity analysis tools in cement and concrete applications, this is the first study to integrate a DRNN model with variance-based sensitivity analysis (VBSA) for pozzolanic concrete. This hybrid framework allows us not only to predict strength with high accuracy, but also to quantify and rank the influence of input variables (e.g., pozzolan type, fineness, admixtures, etc.) on the output in both isolated and interactive contexts.

2.5.3 Large-Scale and Diverse Dataset with Synthetic Augmentation

The current study compiled a unique and comprehensive dataset drawn from 15 different laboratories and augmented it with 3000 synthetically generated samples. This enriched dataset captures a wide spectrum of pozzolanic material behaviors and enables robust model training and sensitivity analysis across diverse conditions, something not addressed in earlier literature that typically relies on small, homogeneous datasets.

2.5.4 Advanced Deep Learning Architecture Tailored for Static Multivariate Inputs

Unlike image or sequence data for which CNNs and LSTMs are naturally suited, the current study involves structured multivariate tabular data. The DRNN architecture was specially tailored with 36 layers, convolutional blocks, and residual connections to effectively handle the nonlinear, high-dimensional relationships in concrete mix design. Further discussion is included in Section 4.1, explaining why

this architecture offers a significant advancement over traditional ANN or shallow DL models.

2.5.5 New Practical Insights from Model-Based Optimization

Beyond modeling accuracy, the current study provides practically relevant recommendations for optimizing mix proportions, pozzolan substitution ratios, and admixture combinations.

2.5.6 Contribution to Sustainable Construction

The current study contributes to sustainability in construction by offering a predictive model to reduce cement content while maintaining performance, and a prescriptive tool to guide eco-friendly mix design decisions. This dual function (prediction + design guidance) makes the presented framework a novel and practical contribution to green concrete technology.

3 Input Data

A comprehensive rationale was followed towards selecting the parameters for the current study. The initial selection of input parameters was based on domain knowledge, an extensive review of the literature, and their physical and chemical relevance to the behavior of pozzolanic cementitious systems. Specifically, factors commonly reported to influence compressive strength are considered, including:

- o Mix proportions (cement, water, sand, gravel),
- o Type and content of pozzolans,
- o Fineness of cement and pozzolans,
- o Type of grinding (inter vs. separate),
- o Use of chemical admixtures (superplasticizers, air-entraining/water-reducing),
- o Specimen dimensions and curing age.

To assess the relative importance of these input parameters, a Variance-Based Sensitivity Analysis (VBSA) was applied, as detailed in Sect. 5.2. This analysis quantifies both the main effect and total effect of each input feature on the predicted compressive strength at 28 and 90 days. Finally, the feature importance derived from the VBSA served not only to justify input selection, but also to optimize mix design in the synthetic data analysis (Sect. 5.3).

The input data for this study were meticulously gathered from previous research conducted across various laboratories (i.e., 15 labs), collectively referred to as X_1 . In particular, lab15 represents the study's results (Müller & Guido, 2016) as the experimental contribution by the authors. The data included 126 different concrete mixtures from different studies using different types of pozzolan, as mentioned in Table 4. This dataset was

Table 4 The labs, number of mixtures, and the used pozzolan of each.

Lab no.	Number of mixtures	Type of pozzolan	Reference
1	4	Basalt	Moawad et al., (2021)
2	4	Basalt with SF	Moawad et al., (2023)
3	10	Volcanic tuffs	Ghiasvand et al., (2014)
4	9	Rhyolite and SF	Eldahroty et al., (2023)
5	11	NP, Perlite, and BFS	Fodil and Mohamed (2018)
6	5	Volcanic ash	Deboucha et al., (2015)
7	16	Pumicite with FA	Mousavinezhad et al., (2023)
8	8	Metakaolin	Paiva et al., (2012)
9	5	Metakaolin	Narmatha and Felixkala (2016)
10	5	Metakaolin	Al-Hashem and et al., (2022)
11	20	Metakaolin	William et al., (2019)
12	5	Metakaolin	Koneru et al., (2023)
13	5	Scoria	Ayene et al., (2023)
14	7	Scoria	Ozvan et al., (2012)
15	12	NP	Hassanein et al., (2022)

systematically organized into six primary categories: mix proportions, types of pozzolan, fineness, additives, grinding type, and specimen dimensions. Additionally, to facilitate comprehensive data analysis, an extra 3,000 sample records were synthetically generated based on the collected data statistics, enriching the dataset and enabling more robust statistical evaluations after the modeling stage.

Table 5 provides a comprehensive overview of the input and output data parameters, detailing each category's associated units, modeled symbols, and statistical ranges, including minimum, maximum, and mean values. For instance, the mix proportions category includes crucial parameters such as gravel content, sand content, water content, and cement content. Each parameter is quantified in kg/m^3 , highlighting the variations in mixture compositions utilized across different studies. Additionally, the pozzolana parameters include both the types and contents of different pozzolans, where X_8 and X_9 represent the quantities of two distinct pozzolana types incorporated in the concrete mix.

The collected data encompassed a wide variety of both natural and artificial pozzolans, which were subsequently coded for model development. The coding scheme is outlined in Table 6, providing clarity on the types of pozzolana incorporated in the analysis and their corresponding codes.

The fineness of both cement and pozzolana is represented in terms of specific surface area (cm^2/gm), with

Table 5 The input and output data nomination.

Category	Input parameter	Unit	Modeled symbol	Range		
				Minimum	Maximum	Mean
Laboratory	Lab no.	—*	X_1	—	—	—
Mix proportions	Gravel content	kg/m ³	X_2	627	1640.27	1014.362
	Sand content	kg/m ³	X_3	204	964	717.43
	Water content	kg/m ³	X_4	101.4	225.26	165.18
	Cement content	kg/m ³	X_5	118.3	620	338.23
Pozzolana	Pozzolana1 type	—	X_{10}	—	—	—
	Pozzolana 2 type	—	X_{11}	—	—	—
	Pozzolana 1 content	kg/m ³	X_8	0	160	45.43
	Pozzolana 2 content	kg/m ³	X_9	0	130	5.83
Fineness	Cement	cm ² /gm	X_{12}	2965	6775	1985.36
	Pozzolana	cm ² /gm	X_{13}	4060	9503	3068.33
Additives	Admixture1	kg/m ³	X_6	0	13.5	2.73
	Admixture2	kg/m ³	X_7	0	10	0.47
Grinding type	Inter/separate	—	X_{15}	—	—	—
Specimen	Dimensions	—	X_{14}	—	—	—
Output variable	Compressive strength at 28_days	MPa	Y_1	14.94	95.33	43.46
	Compressive strength at 90_days	MPa	Y_2	19.54	88.5	27.24

* Integer variable

Table 6 Pozzolan type and its entered code.

Pozzolan type	Pozzolan code
Basalt	1
Volcanic tuff	2
Rhyolite	3
Natural pozzolan	4
Perlite	5
Volcanic ash	6
Pumicite	7
Metakaolin	8
Scoria	9
Silica fume	10
Blast furnace slag	11

Table 7 The entered nomination for the fineness values.

Component	Fineness (cm ² /gm)		
Cement	<3500	3500:5000	>5000
Pozzolan	<5000	5000:7900	≥8000
Entered value expression	1	2	3

its values assigned coded numbers for ease of analysis. Table 7 shows the fineness classification of cement and pozzolana according to the specified requirements. To further understand how fineness might affect the

material qualities and performance of the finished concrete, this chart categorizes fineness into three separate levels. There are three distinct ranges for cement fineness, defined by specific surface area: below 3500 cm²/gm, between 3500 and 5000 cm²/gm, and over 5000 cm²/gm. In the same way, pozzolana fineness is classified as follows: less than 5000 cm²/gm, between 5000 and 7900 cm²/gm, and equal to or higher than 8000 cm²/gm. Using this categorization, we can better grasp how varying degrees of fineness impact the pozzolanic reactivity and general performance of concrete mixes.

Two types of admixtures were included in the parameters: admixture 1 represented different types of superplasticizers, and admixture 2 represented additional types of admixtures (water-reducing or air-entraining) used with the superplasticizers.

Finally, the compressive strengths at 28 and 90 days, Y_1 and Y_2 , respectively, are the outcome variables of importance in this investigation. These variables serve as essential performance indicators for the pozzolanic concrete being studied, allowing a comprehensive evaluation of the impact of different input parameters on strength development over time.

As a first step toward further study, this thorough data collection and classification will allow us to understand better how various mix components affect the compressive strength of pozzolanic concrete.

During preprocessing, we applied both statistical and domain-based outlier detection techniques. Z-score

filtering was used to flag values beyond ± 3 standard deviations from the mean, and they were carefully reviewed. Flagged values were cross-checked against known physical limits and published ranges in pozzolanic concrete literature. For example, excessively high or low water-to-cement ratios or unrealistic pozzolan contents were identified, excluded, or corrected. Finally, scatter plots and histograms were used to further confirm the removal of spurious entries before training the model. Only data points that passed both statistical and engineering plausibility checks were retained for model training and validation. To address potential inconsistencies, biases, and the data preprocessing steps applied to ensure dataset integrity, particular precautions are considered in the current study and summarized as follows:

- The compiled dataset consists of experimental data from 15 different laboratories (as indicated in Table 4), each contributing unique pozzolanic concrete mix compositions and test results. Recognizing the potential variability in measurement techniques, units, and mix design practices across these sources, a multi-level consistency verification procedure was applied, including: standardizing units (e.g., kg/m³ for all material quantities, cm²/g for fineness), harmonizing age categories for compressive strength (e.g., interpolating missing values to unify 28-day and 90-day datasets) and cross-validating outlier values against reported literature ranges to flag potential errors.
- Since the datasets sourced from different studies may be skewed toward specific pozzolan types, curing conditions, or strength classes, particular steps were implemented to mitigate these biases, including: augmented the dataset with 3,000 synthetic samples generated using statistical distributions derived from the collected data, and applied data normalization and encoding techniques, especially for categorical variables like pozzolan type and grinding method, to ensure equitable representation during model training.
- Instances of missing or incomplete entries were carefully addressed: first, imposition using domain-specific heuristics (e.g., inferring water content based on known water–cement ratios). Second, the exclusion of records with critical missing or inconsistent fields that could not be reliably estimated. After cleaning, only records with complete and validated parameter sets were included in the modeling phase, ensuring the model was trained on high-quality, consistent data.
- The effectiveness of these cleaning and standardization steps was validated through: goodness-of-fit evaluation of the DRNN model, which showed minimal overfitting and balanced error distributions (see

Fig. 10). Error independence and normality confirmation via line-of-equality (LOE) and residual plots. Reproduction of known experimental trends (e.g., the effect of pozzolan type and fineness on the strength) in the synthetic data analysis (Sect. 5.3), affirming the internal consistency of the dataset.

4 Analysis Framework

The developed framework comprises four main steps: data preparation, modeling, testing, and post-processing analysis. In the first step, the data are prepared, and the relevant components and their respective domain areas are identified, as described in Sect. 3. The second step involves processing the literature data categories, after which the combined data are input into the DRNNs model, leaving out testing data used to assess the model's transfer learning capability across different labs. The third step focuses on testing the model using various goodness-of-fit metrics to establish confidence in the GSA. In the final step, the model is used to forecast compressive strength values for a broad range of synthetically generated input data based on the predefined factors domain (i.e., input data description). The post-processing tool, VBSA, generates sensitivity results/indices. These phases are illustrated in the general workflow presented in Fig. 7.

4.1 Machine Learning Technology

ML emerged as a subfield of artificial intelligence in the 1990s. Unlike symbolic approaches, it utilizes statistical and probabilistic models and tools (Langley, 2011; Rosenthal, 2003). In essence, ML enables computers to learn to perform specific tasks by analyzing large datasets (Dietterich, 2000; Müller & Guido, 2016). Before applying these methods, a step called feature extraction is necessary to identify the characteristics that provide the most relevant information. The sample data are then used to train the system to recognize features and discern patterns (Avci et al., 2021; Haenlein & Kaplan, 2019; Marani & Nehdi, 2020). Deep Learning (DL) methods were introduced to overcome the limitations of manually designed features in complex ML applications (Avci et al., 2021; Owais, 2024b). DL is inspired by discoveries in neuroscience and mimics how the nervous system processes and communicates information. DL layers consist of hidden layers in an artificial neural network and involve advanced algorithms.

Furthermore, based on training data, ML can be classified as supervised, unsupervised, semi-supervised, or reinforcement learning (Alpaydin, 2020; Ivanovic & Radovanovic, 2015). Supervised and unsupervised learning are the most widely used types of machine learning,

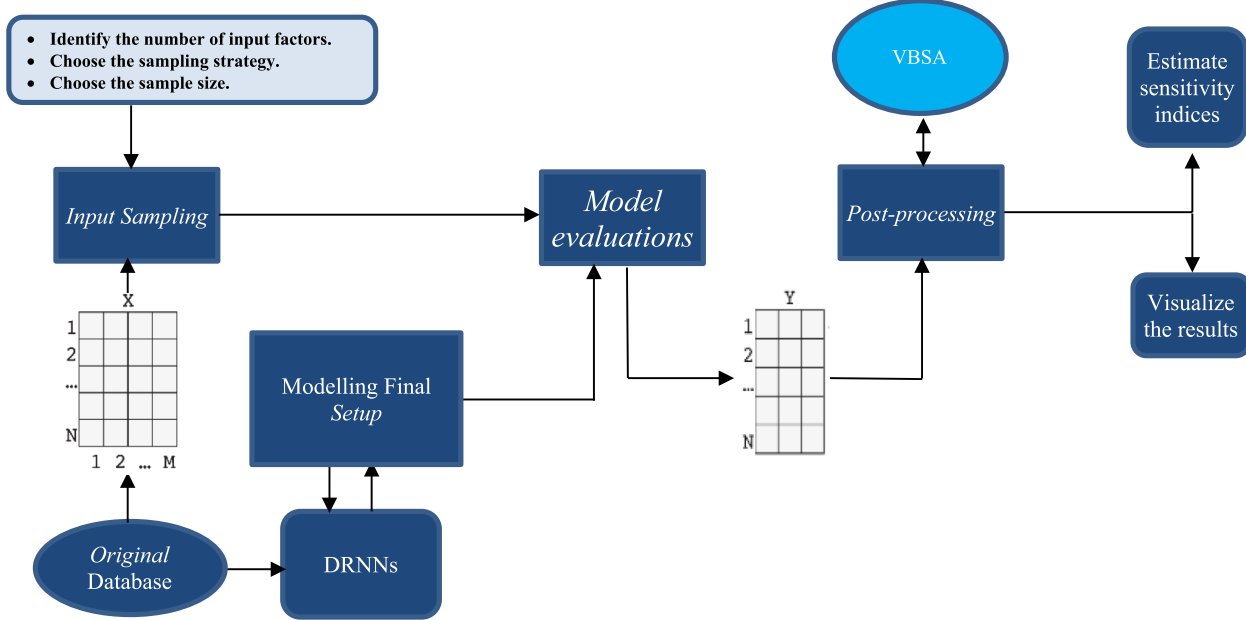


Fig. 7 The framework of analyzing PzC concrete mixtures.

especially in engineering (Almutairi & Owais, 2025; Taffese & Sistonen, 2017). In supervised learning, the system learns from a dataset containing both input values and their corresponding outputs, allowing it to predict future outcomes based on this relationship. On the other hand, unsupervised learning involves datasets where only the inputs are known, and the system must find patterns or predict outputs without explicit guidance (Taffese et al., 2015). The modeling conducted in this study falls under supervised learning.

DL techniques, specifically Deep Neural Networks, were developed to address the limitations of hand-crafted features in advanced ML systems (Avci et al., 2021; Haenlein & Kaplan, 2019). DL models can automatically connect features to desired outputs and perform feature extraction (Schmidhuber, 2015). With adequate training, DL systems can directly map raw inputs to target outputs without needing explicit feature extraction, and they can identify hierarchical abstract features that explain simpler learned patterns (Owais & Sayed, 2025). This allows DL algorithms to break down complex tasks into manageable problems and solve them effectively (Owais, 2024a).

The compressive strength of PzC concrete mixtures is a complex phenomenon influenced by numerous factors with highly correlated interactions. To model this complexity, convolution layers are utilized in this work. The developed framework aims to uncover latent connections between input and output variables while achieving optimal prediction accuracy. Reference Du et al., (2016) introduced the Residual Network (ResNet) concept to the

DL framework to improve gradient propagation in very deep networks and resolve associated challenges. ResNet uses shortcut connections that bypass several network layers, allowing high-accuracy training and enabling layers to learn residual functions from layer inputs rather than unrelated functions (Almutairi & Owais, 2024; Alshehri et al., 2023). This concept is applied in this work using Deep Residual Neural Networks (DRNNs).

The depth of the DRNNs used is set at 36 layers, divided into three main sections:

- The first section includes an input layer with a convolutional layer (CL), a rectified linear unit activation layer (ReLU), and a batch normalization layer (BNL).
- The second section consists of a stack of four Residual Building Units (ResBU), which form the core of the structure.
- The final section contains three layers: a fully connected layer (FCL), a Softmax layer, and an output layer.

The first layer normalizes the input data before passing it into the network. This normalization process adjusts the incoming data by subtracting the mean values. Table 8 provides the mathematical notations used in the proposed DRNNs, highlighting their key functions. The controlling functions are as follows:

$$H_{l+1} = \text{ReLU}[f(H_l) + id(H_l)], \quad (1)$$

Table 8 Nomenclature.

Symbol	Definition
H_{l+1}	Is the output of the l^{th} resbu
$id(H_l)$	Is the identity function
H_l	Is the input of the l^{th} resbu
$f(H_l)$	Is the residual function
c_j	Is the batch input value
\hat{c}_i	Is the normalized activation value
\bar{y}_p	Is the mean of the predicted compressive strength values
\bar{y}_m	Is the mean of the measured compressive strength values
y	Is compressive strength after 28 days
ϵ	Is an Epsilon attribute
β	Is a learnable offset
μ_B	Is the mini-batch mean
σ_B^2	Is the mini-batch variance
n	Is the number of total data points
p	Is a subscript that denotes predicted values
m	Is a subscript that denotes measured values
z_j	Is the input values of the Softmax layer
γ	Is a learnable scale factor
r	Is the sequence length
t	Is the number of testing data points

$$\hat{c}_i = \left(\frac{(c_j - \mu_B)}{\sqrt{(\sigma_B^2 + \epsilon)}} \right), \quad (2)$$

$$z_j = \gamma \hat{c}_i + \beta, \quad (3)$$

$$\text{Relu}(z_j) = \begin{cases} 0, & z_j < 0 \\ z_j, & z_j \geq 0 \end{cases}, \quad (4)$$

$$f(z_j) = \frac{e^{z_j}}{\sum_{j=1}^K e^{z_j}}, \quad (5)$$

$$\text{Loss} = \frac{1}{r} \sum_{i=1}^r \left[\sum_{j=1}^t (y_{pj} - y_{mj})^2 \right], \quad (6)$$

$$\text{MSE} = \frac{\sum_{j=1}^t (y_{pj} - y_{mj})^2}{t}. \quad (7)$$

Each Residual Building Unit (ResBU) in the proposed framework is composed of two parts: the main branch and the residual branch. The main branch contains six layers: two convolution layers (CL), two rectified linear unit (ReLU) activations, and two batch normalization layers (BNL). The BNL serves as an intermediary

between the CL and the ReLU, maintaining this structure consistently throughout the Deep Residual Neural Networks (DRNNs). The residual branch, functioning as a shortcut, bypasses the first five layers of the main branch (i.e., CL-BNL-ReLU-CL-BNL), connecting directly before the final ReLU. The main branch then incorporates the output of the residual branch through an elementwise addition before the final activation layer. The computations within each ResBU follow Eq. (1). Interestingly, the identity function ($id(H_l)$) in the shortcut path does not add any computational burden but ensures a smoother gradient flow (Du et al., 2016; Owais et al., 2020a).

As illustrated in Fig. 8a, each ResBU includes both a main and a residual branch. In the main branch, each convolutional layer is followed by a BNL and a ReLU activation. The shortcut in the residual branch allows input values to bypass the main branch's layers and connect directly to the final ReLU layer, as shown in Fig. 8b. The residual output is combined with the main output before the final activation layer. This configuration ensures efficient gradient propagation without increasing the computational complexity (Du et al., 2016).

The convolution layers (CL) perform their task by applying filters over the input data, learning internal features through these filters, which extract local patterns. The CL generates feature maps using sliding filters that compute the dot product of their respective weights, inputs, and biases (Zang et al., 2018). Following this, the BNL regularizes the output to prevent overfitting (Ioffe & Szegedy, 1502). Additionally, the BNL accelerates the training process by normalizing and reorienting each input channel, improving the model's robustness and reducing sensitivity to initialization (Goodfellow et al., 2016). Equation (3) governs the mini-batch scaling and shifting process in the BNL, where learnable parameters (γ and β) adjust the scaling, and the epsilon value (ϵ) ensures numerical stability during training (Almutairi et al., 2024).

The output from the BNL is passed through the ReLU activation, which introduces non-linearity and enables the network to learn complex representations (Szegedy, et al., 2015). Equation (4) applies the ReLU function to each input element (z_j), preventing negative values while maintaining the input size. ReLU was chosen for its superior performance compared to other activation functions like hyperbolic tangent or sigmoid, allowing for faster training and more accurate generalization without requiring extensive deep-learning iterations (Owais et al., 2020b; Ramachandran et al., 1710).

In the fully connected layer (FCL), all neurons are connected in an all-to-all manner with the preceding layer, allowing the network to utilize all previously

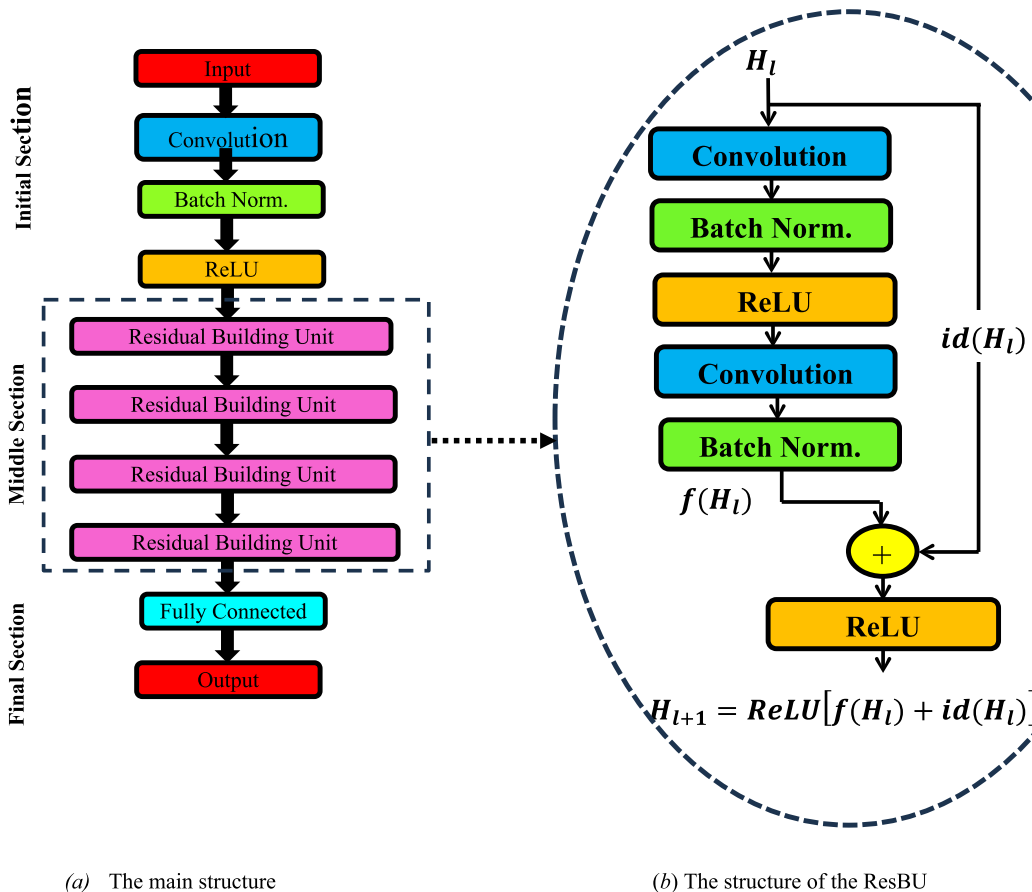


Fig. 8 The employed DRNNs structure.

learned features for the most accurate predictions (Goodfellow et al., 2016; Owais et al., 2019). The FCL is linked to the Softmax layer, which calculates the probability distribution of the predicted compressive strength values. The Softmax function, described by Eq. (5), is a normalized exponential function used for multi-class classification. It generalizes the logistic sigmoid function for this purpose (Bishop, 2006).

Finally, at the output layer, the model's performance is measured using the loss function and mean-squared error (MSE), calculated by Eqs. (6) and (7). These metrics help adjust the difference between predicted and actual compressive strength values. During the training process, 36 filters of size four are applied in each CL, generating 36 feature maps. A mini-batch size of 256 is used, employing the stochastic gradient descent algorithm, which is optimal for weight initialization, particularly in networks using ReLU layers (He et al., 2015; Owais, 2024c).

4.2 Goodness-of-Fit Statistics

The DRNNs model employed in this study is considered valuable as it offers an alternative to the

physical laboratory processes for conducting various experiments using the GSA procedure. Replacing these experimental setups with a numerical model for predicting the compressive strength of PzC concrete mixtures can be especially useful, given that the VBSA approach requires numerous samples to achieve convergence (as shown in the results section). The importance of goodness-of-fit metrics is emphasized since the reliability of VBSA conclusions is contingent upon these values. The literature presents many such metrics, each assessing model accuracy differently (Owais & Alshehri, 2020).

Coefficient of determination (R^2), root mean square error (RMSE), mean absolute percentage error (MAPE), and residual plots are some of the well-established performance measures utilized to assess the model's predictions in this study (Pellinen, 2002). For every model, these metrics may be computed separately. The correlation between anticipated and observed values, denoted by R^2 , is calculated using the following equation:

$$R^2 = 1 - \frac{\sum_{i=1}^n (y_{pi} - y_{mi})^2}{\sum_{i=1}^n (y_{mi} - \bar{y}_m)^2}. \quad (8)$$

Relying on a single accuracy metric (e.g., R^2) may be misleading, as it does not comprehensively assess model performance. Therefore, using a combination of accuracy metrics is crucial for drawing reliable conclusions about model behavior. Additional global bias indicators should be examined to assess model bias. The line-of-equality (LOE) plot, which displays the difference between the observed and predicted values, is handy for this purpose. Ideally, this plot shows a random distribution of points with constant width around the LOE. This tool helps check whether the model meets assumptions of constant variance, normality, and independence of errors (Hussain & Akbar, 2022; Tsai et al., 1998).

The root mean square error (RMSE) is a quadratic scoring method that reflects the average magnitude of prediction errors, while MAPE is a linear metric that assigns equal importance to all individual deviations from the mean error (Owais et al., 2021). Both RMSE and MAPE are used in this study to assess the deviations between predicted and actual values, with their calculations shown below:

$$RMSE = \sqrt{\frac{\sum_{i=1}^n (\frac{y_{mi} - y_{pi}}{y_{mi}})^2}{n}} \times 100, \quad (9)$$

$$MAPE = \frac{\sum_{i=1}^n \left| \frac{y_{mi} - y_{pi}}{y_{mi}} \right|}{n} \times 100. \quad (10)$$

These collective metrics provide a thorough evaluation of model performance, enabling more accurate predictions and reliable conclusions regarding the behavior of PzC concrete mixtures.

4.3 Variance-Based GSA

While DL methods are powerful tools for making predictions, they often lack transparency when understanding the underlying relationships in their models, making interpretation difficult (Jiang et al., 2020). To address this issue, sensitivity analysis (SA) can be employed to clarify the cause-and-effect dynamics between inputs and outputs of a trained DRNNs model. This section introduces the VBSA for predicting the compressive strength of PzC concrete mixtures. Integrating VBSA into the analysis enables a more comprehensive understanding of the relationships between the input factors and the predicted compressive strength. Additionally, it allows for the

quantitative evaluation of how much each input variable contributes to the final prediction.

To reduce the need for extensive experimental testing, a model-based approach is proposed, which involves calculating the partial derivatives as follows:

$$\begin{aligned} & \text{Compressivestrength after 28/90 days} \rightarrow y \\ & = f(x_1, x_2, \dots, x_i, \dots, x_k) : Rk \rightarrow RSi = \frac{\partial y}{\partial x_i}, \forall X. \end{aligned} \quad (11)$$

In this equation, S_i represents the sensitivity index, which indicates the significance of the input variable x_i in determining the value of y . However, the local sensitivity analysis (LSA) approach has two key limitations: some models may not be differentiable, and the sensitivity index can give misleading results when the input variables are highly correlated. This method also relies on strong assumptions regarding model normality, linearity, and monotonicity, making it unsuitable for more complex models.

To overcome these challenges, VBSA was developed. Unlike LSA, VBSA analyzes a global set of samples, accounting for variable interactions (joint effects) among the input variables. Its variance-based form produces robust sensitivity indices across the entire input domain, capturing the influence of each input factor while allowing all others to vary (Owais & Matouk, 2021; Saisana et al., 2005). In the context of the complex DRNN model used in this study, VBSA provides a deep insight into how multiple intercorrelated variables interact with the output. Two primary indices are used in VBSA to evaluate the importance of the input factors (Saltelli et al., 2006):

$$S_i^f = \frac{V_{x_i}[E_{X_{\sim i}}(y/x_i)]}{V[y]}, \forall x_i, \quad (12)$$

$$S_i^T = \frac{E_{X_{\sim i}}(V_{x_i}[y/X_{\sim i}])}{V[y]}, \forall x_i. \quad (13)$$

In these equations, x_i is the input variable under analysis, and $X_{\sim i}$ refers to all other variables except x_i . Equation (12) defines the first-order sensitivity index (S_i^f), which measures the contribution of x_i to the total variance of y without accounting for interactions with other variables. Meanwhile, Eq. (13) calculates the total sensitivity index (S_i^T), which includes both the direct and interactive effects of x_i on y . Both indices range from 0 to 1, where 1 indicates that the variable fully explains the variation in y , and 0 implies no influence on the outcome. The first-order index (S_i^f) helps rank the significance of input variables, but a low value should not automatically dismiss the variable as unimportant. Instead, the total

effect index (S_i^f) is a more reliable indicator of whether a variable impacts the output (Owais et al., 2013).

In practice, probability density functions are assigned to each variable to calculate these indices. Fortunately, the precise representation provided by the DRNNs enables high-confidence sensitivity analysis using Latin hypercube sampling (LHS), which explores the entire input space (Saltelli et al., 2006). The VBSA-LHS process can be summarized as follows:

Generate a sample matrix T :

$$T = \begin{pmatrix} x_{11} & x_{12} & \dots & x_{1i} & x_{1k} \\ x_{21} & x_{22} & & x_{2i} & k \\ \vdots & \vdots & \ddots & \vdots & \vdots \\ x_{\mu 1} & x_{\mu 2} & \dots & x_{\mu i} & x_{\mu k} \end{pmatrix}. \quad (14)$$

- Here, k is the number of input variables, and μ is the sample size. Each row represents an experiment from the LHS trials.
- Divide the sample matrix T into two equal parts: A and B .
- Create a new matrix \bar{B} by replacing the x_i column in B with the corresponding column from A .
- Compute the output vectors Y using the DRNN model:

$$YA = \begin{pmatrix} y^1 \\ y^2 \\ \vdots \\ y^{\mu/2} \end{pmatrix} \& Y^{\bar{B}} = \begin{pmatrix} y^{\frac{\mu}{2}} \\ y^{\frac{\mu}{2}+1} \\ \vdots \\ y^{\mu} \end{pmatrix}. \quad (15)$$

Finally, calculate the first-order (S_i^f) and total (S_i^T) sensitivity indices for each variable as follows:

$$S_i^f = \frac{\frac{2}{\mu} Y^A \cdot Y^{\bar{B}} - E(Y^A)^2}{Var(Y^A)}, \quad (16)$$

$$S_i^T = 1 - \frac{\frac{2}{\mu} Y^B \cdot Y^{\bar{B}} + E(Y^A)^2}{Var(Y^A)}. \quad (17)$$

The purpose of Eqs. (14–17) is to average the effects of all input variables to determine their global impact on the response variable. It's important to note that the first-order sensitivity (S_i^f) represents the effect of a variable when all others are held constant (OAT). Conversely, the total sensitivity (S_i^T) captures the variable's impact when others are allowed to vary (AAT). If the relationships between the variables are linear and independent, the two indices will yield similar values. However, this averaging method is crucial because the model does not guarantee linearity, monotonicity, or independence. It

is also essential to select an adequate sample size μ to ensure that the variance and covariance are properly represented, and adjustments to this value will be discussed in the subsequent section.

5 Numerical Study

5.1 Evaluation of DRNNs

The methods developed in this study were implemented using MATLAB 2021a on a personal computer equipped with a 2.6 GHz Intel® Xeon® CPU, 64 GB of RAM, and a GeForce GTX 1050 graphics card. The input and output data from the literature database were normalized for use in the proposed DRNNs architecture.

The model validation procedures were carefully designed to ensure the robustness, accuracy, and generalizability of the Deep Recurrent Neural Network (DRNN) model. These procedures included a combination of train–test splitting, cross-validation, overfitting prevention techniques, and tests for model generalizability, including transfer learning capabilities.

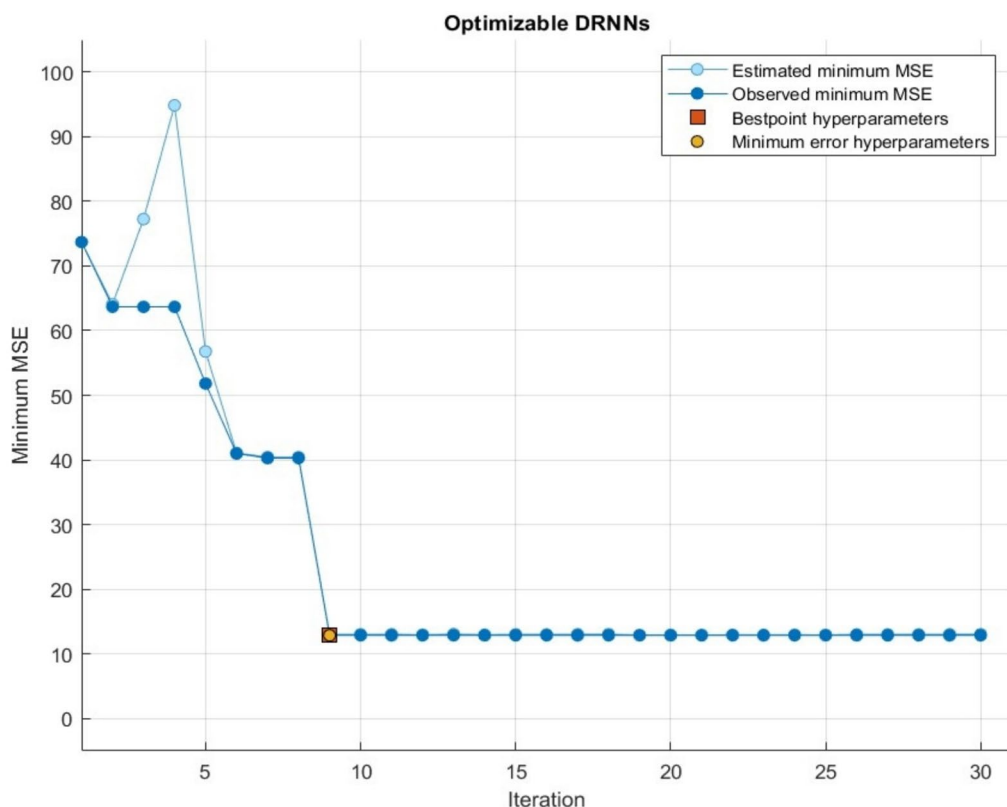
To begin, the dataset was divided using a standard 80/20 train–test split. In this setup, 80% of the data was allocated for training the DRNN model, while the remaining 20% was set aside for independent testing. This division was performed randomly to minimize any selection bias and to ensure that the test subset accurately represented the full distribution of the input parameters. Such a random partitioning helps in producing more realistic and reliable estimates of model performance on unseen data.

In addition to the initial train–test split, a fivefold cross-validation strategy was employed during the hyperparameter tuning phase to enhance the evaluation rigor. This approach involved dividing the training data into five equal folds, iteratively using four folds for training and one for validation. This method ensured that the model's performance was not dependent on any single data partition and allowed for the assessment of consistency across multiple data subsets. The results showed a stable performance, with R^2 values consistently ranging from 0.91 to 0.94 and RMSE variations within acceptable limits, highlighting the model's robustness and reliability.

To guard against overfitting—a common issue in deep learning models—several strategies were implemented. First, residual analysis was conducted, and as illustrated in Fig. 10, the residual plots showed normally distributed and independent errors for both training and testing data, with no noticeable trends or clustering. This suggested a well-fitted model without signs of overfitting. Furthermore, batch normalization layers were integrated throughout the DRNN architecture to regularize the training process, reduce variance, and improve model

Table 9 Goodness-of-fit statistics of average DRNNs predictions compared with different ML tools.

Model	Training data			Testing data		
	R^2	RMSE%	MAPE%	R^2	RMSE%	MAPE%
MLR	0.75	13.34	10.56	0.72	17	12.22
ANN	0.86	6.87	5.43	0.84	8.45	5.73
SVM	0.88	4.45	3.68	0.88	5.67	3.88
REPTree	0.92	3.33	2.42	0.90	3.98	3.20
CNNs	0.93	3.12	2.34	0.92	3.89	3.11
LSTMs	0.93	3.13	2.35	0.90	3.99	3.22
DRNNs	0.95	3.02	2.76	0.94	3.26	2.96

**Fig. 9** Optimizing process of DRNNs hyperparameters.

generalization. Finally, the close alignment of performance metrics such as R^2 , RMSE, and MAPE across both training and testing sets indicated that the model successfully captured generalizable patterns rather than overfitting to the training data.

Lastly, the model's generalizability and transfer learning capabilities were critically evaluated. One of the major strengths of the proposed framework lies in its capacity to generalize across a broad range of experimental conditions, supported by the diverse data collected from

15 different laboratories. To rigorously test this capability, the testing phase was designed to include scenarios where lab-specific data were withheld from training and later used to evaluate transfer learning performance. The results, summarized in Table 9, demonstrated that the model maintained high predictive accuracy even on previously unseen data, thereby confirming its strong generalization and transfer learning potential.

During the parameter tuning and training process for the DRNNs model, each convolutional layer (Conv)

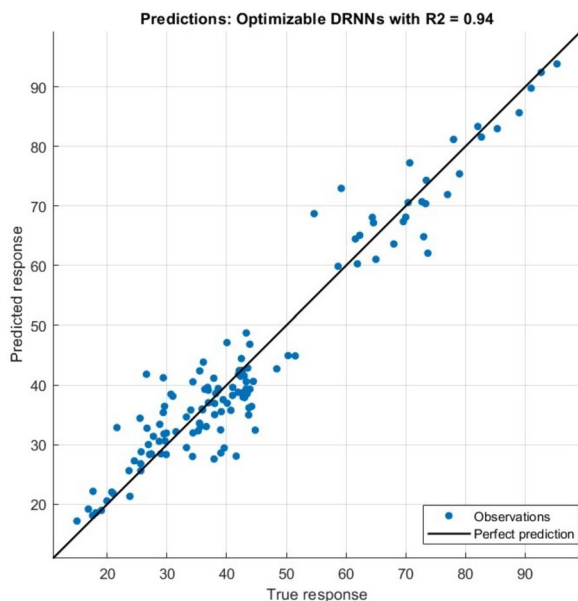


Fig. 10 True values vs. DRNNs prediction values.

generated 30 feature maps using kernels of size four. The stochastic gradient descent algorithm was employed with a mini-batch size of 128. The initial learning rate was set to 0.02 for weight initialization and decayed exponentially to 0.005 after 30 epochs. As illustrated in Fig. 9, these parameters were optimized during early hyperparameter tuning. Figure 10 demonstrates the accuracy of the DRNNs predictions when compared to the actual data, showcasing the model's ability to capture the high variance in compressive strength as the target output.

A multi-criteria evaluation was conducted, comparing the DRNNs with other ML methods. However, a direct comparison to reported accuracies in the literature is considered unfair due to the uniqueness of the collected data. Table 9 highlights the strong performance of the DRNNs across various metrics, as discussed in the goodness-of-fit section when compared to the best-performing ML methods applied to the same data set. Although models such as Convolutional Neural Networks (CNNs), Long Short-Term Memory networks (LSTMs), and Deep Residual Neural Networks (DRNNs) fall under the broader category of deep neural networks, DRNNs are uniquely suited for modeling problems with complex, nonlinear dependencies and a relatively structured but static input space such as ours. CNNs are highly effective in spatial feature extraction (e.g., images), and LSTMs excel in temporal sequence modeling. However, the compressive strength prediction task addressed in this study involves neither image data nor time-series patterns but rather tabular multivariate inputs with

high-dimensional interactions between physical and chemical features of concrete mix components.

DRNNs offer a distinct advantage due to their ability to mitigate the vanishing gradient problem in deep networks using shortcut (residual) connections. This enables deeper architectures to learn complex relationships without degradation in performance. The residual units allowed the network to retain important low-level features while capturing deeper nonlinear patterns, which are essential for modeling material behavior.

To validate this, a benchmarking study was included in Table 9, where the performance of DRNNs is compared to CNNs and LSTMs on the same dataset. The results showed that DRNNs achieved a higher R^2 value, lower RMSE, and more stable residual error distribution compared to both CNNs and LSTMs. These outcomes confirm that DRNNs are better suited for this type of material-property prediction problem.

The similar accuracy between the training and testing phases confirms that the model learned the underlying patterns without overfitting the data. Model bias was further evaluated using data distribution around the LOE in Fig. 10, which indicated a normal error distribution and evidence of error independence. These validation steps are crucial for ensuring that the DRNNs effectively capture the relationships between the input parameters and the output. If the model accurately learns the latent features of PzC concrete mixture components and their role in determining compressive strength, the VBSA could reliably identify the most important input factors.

5.2 VBSA Results

After validating the DRNNs model, it is now ready for the VBSA analysis. The model examines k input components, each divided into ϕ levels, creating a grid of ϕk -by- ϕk prediction points. In this case, with up to eleven input components and ten values each, around eleven trillion points are evaluated. To determine the number of samples required, two approaches can be used: deterministic and stochastic. Deterministic sampling systematically selects μ samples to uniformly cover the entire domain, ensuring all areas are represented. On the other hand, stochastic methods treat input data as random variables with defined probability density functions (PDFs) and generate μ samples accordingly. In this study, Latin Hypercube Sampling (LHS) with a deterministic approach was applied to align with the fixed mixing design and environmental conditions of PzC concrete mixtures.

LHS is a statistical method used to generate samples from a quasi-random multivariate distribution, ensuring each sample appears uniquely positioned across all

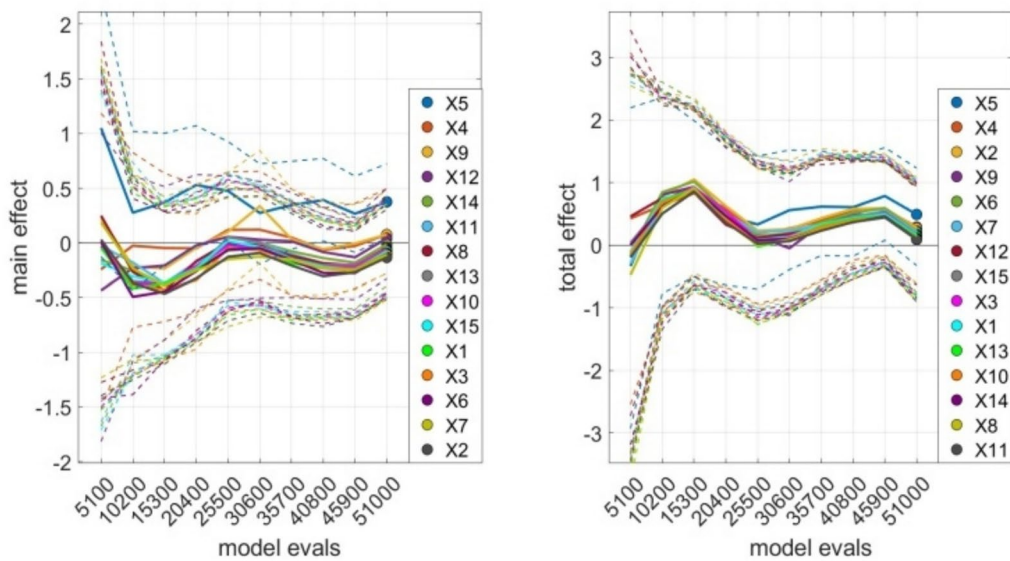


Fig. 11 Total order and main effect indices convergence diagrams.

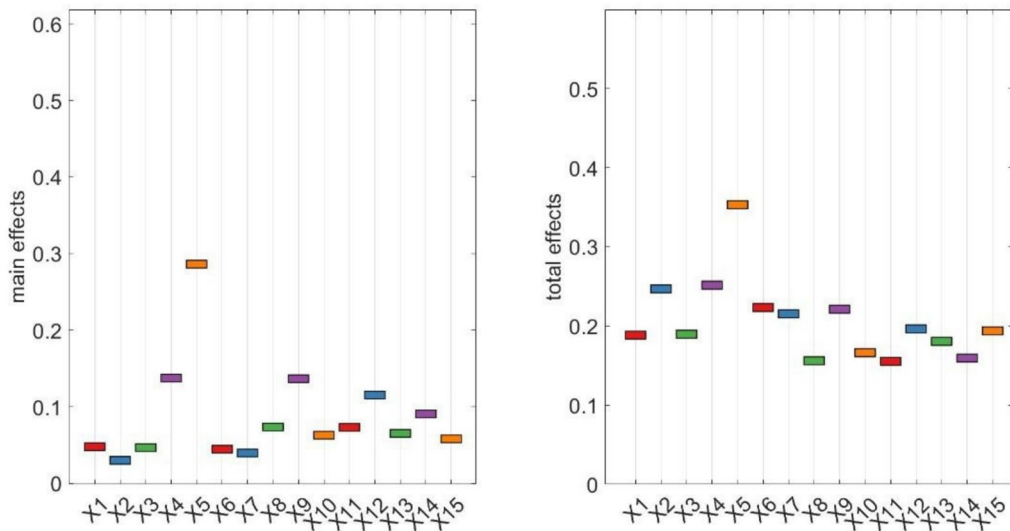


Fig. 12 Prioritization of parameters by main and total effects after 28 days.

axes. When sampling a function with n variables, each variable's range is divided into ϕ intervals with equal probability, meeting the requirements of the LHS method. One key advantage of this approach is the independence of the sampling process, allowing random samples to be collected sequentially without overlap. Another benefit is the ability to track which samples have already been used, ensuring efficient sample collection.

The accuracy of VBSA indices increases with the sample size μ , though available computational resources

limit it. The challenge lies in determining the appropriate number of evaluations necessary for reliable sensitivity indices. As shown in Fig. 11, sensitivity indices stabilize as the sample size increases, and a sample size of 51,000 was sufficient for the main and total effect indices to converge.

The VBSA plays a crucial role in ranking the parameters based on their impact on compressive strength, both independently and in combination with other variables. The VBSA clearly highlights each parameter's impact on

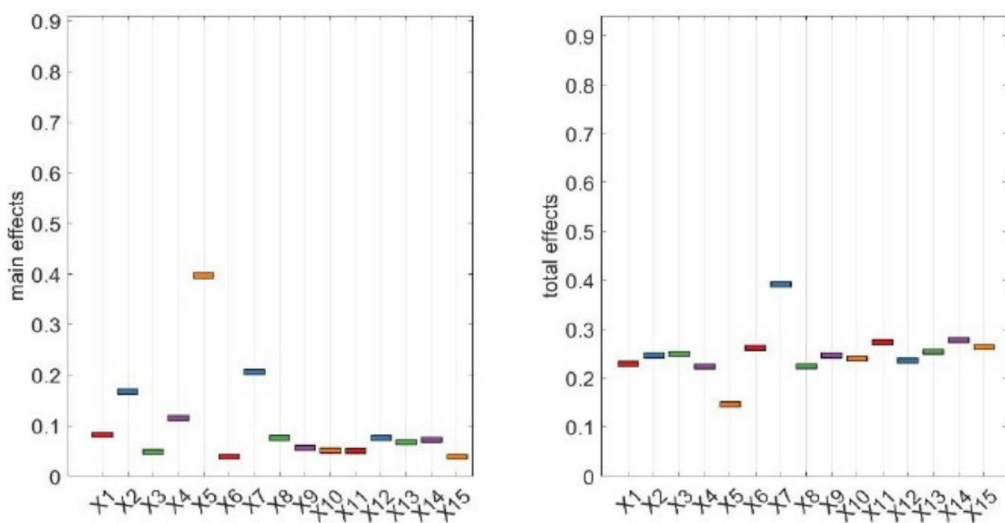


Fig. 13 Main and total effects on compressive strength after 90 days.

the compressive strength of concrete, both as an independent (main effect) and in combination with other factors (total effect), measured after 28 and 90 days. The model generated numerous hypothetical records to identify the general behavior of each parameter, as shown in Fig. 11. Figure 12 indicates that cement content emerged as the most influential factor in compressive strength after 28 days, whether or not other parameters were considered. The significance of other factors, such as gravel and water content, the presence of admixtures, and the use of an additional pozzolan, became more apparent when considering their interactions. These factors showed promising effects when evaluated together. Also, Fig. 12 shows that the ranking of parameters based on their main effect differs from their ranking based on total effect, except for cement and water content, which consistently showed the most significant influence on compressive strength. Even with extensive sampling, gravel content, additional pozzolan, and two types of admixtures had notable effects when accounting for interactions with other parameters.

Over time, in concrete curing, the prioritization of these parameters shifted. As depicted in Fig. 13, cement content remained the most significant factor when its main effect was isolated, while using additional admixtures showed the most substantial impact when considering other variables. Though pozzolan content had minimal main effect, it exhibited a robust total effect when used in combination with other parameters, especially when two types of pozzolan were used. Similarly, the fineness of cement and pozzolan, along with the grinding type, had significant total effects.

Comparing the total effects after 28 and 90 days revealed that factors such as grinding type, fineness, pozzolan type, pozzolan content, and the use of admixtures—particularly when two types were used—became more pronounced over time. Figure 14 demonstrates the contributions of each parameter to the increase in compressive strength from 28 to 90 days. Cement and gravel content, combined with using two admixtures, were key contributors to this increase. The effect of cement fineness also became evident over time.

As can be interpreted, VBSA calculates both main effect indices (first-order sensitivity) that reflect the isolated contribution of each input factor to output variance, and the total effect indices, which include interaction effects, i.e., how a variable contributes in combination with others. By comparing the differences between these two, we identified variables with strong synergistic behavior, even if their main effects were moderate or low. For instance, the second pozzolan type showed a low main effect but a high total effect, indicating that its influence is primarily through interactions with other mix components (e.g., cement content, pozzolan fineness). Admixtures, especially when combined (superplasticizer + secondary admixture), display enhanced interaction effects with water content and cement fineness. The cement and water contents clearly influence workability and strength balance, with total effects higher than the sum of their individual main effects. Finer pozzolans, particularly when used in combination (e.g., silica fume + metakaolin), showed enhanced strength outcomes, suggesting synergistic reactivity. Although grinding type had limited impact in isolation, its

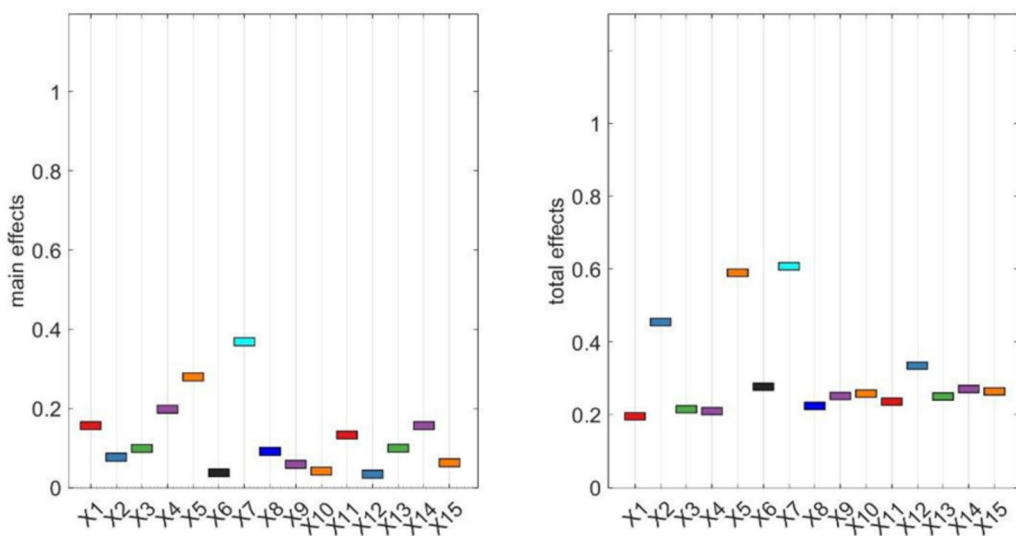


Fig. 14 Main and total effects on compressive strength increase from 28 to 90 days.

interaction with pozzolan fineness and cement content had notable effects on early strength development.

5.3 Synthetic Data Analysis

As mentioned before, an additional 3,000 synthetic data records are generated to allow for a more in-depth exploration of how the main program categories impact compressive strength. Each mix component exhibited an optimal weight range that contributed to higher compressive strength values. Figure 15 presents the optimal weight range for each component as determined by the model.

The analysis revealed the expected optimal absolute weights for the components of pozzolanic concrete mixtures: sand (400–650 kg/m³), gravel (900–1011 kg/m³), superplasticizer (13 kg/m³), additional admixture (if present, 10 kg/m³), water/cement ratio (0.5–0.6 for normal concrete and less than 0.4 for high-strength concrete), and pozzolan content (100–150 kg/m³). These values were found to be optimal for achieving high compressive strength. Some high-strength predictions at elevated w/c ratios reflect model-inferred outcomes based on multi-factor interactions in the synthetic dataset and should be interpreted cautiously, considering potential extrapolation effects beyond the range of typical experimental observations. Figure 16 demonstrates that the higher the cement content, the higher the compressive strength. Based on the input data, most studies indicated that compressive strength often surpassed the specified design strength. Consequently, reducing the cement content might be advisable to meet the required strength more precisely. Only about 15% of the input records met

the specified design strength without significant excess. For instance, the lowest pozzolanic cement content required to achieve 25 MPa after 28 days was 259 kg/m³ if 30% of cement was replaced by scoria (Rosental, 2003) and 272 kg/m³ if 15% of cement was replaced by basalt (Moawad et al., 2021).

The type and content of pozzolan also significantly influenced compressive strength, as shown in Fig. 17. The analysis reveals that mixtures including silica fume and volcanic ash consistently produced higher predicted compressive strength values across different optimal ranges (i.e., 100–150 kg/m³ substitution levels) (Eldaheraty et al., 2023). Some natural pozzolans demonstrated compressive strength values close to those achieved by artificial pozzolans, making local availability a key factor in pozzolan selection.

The model found that a pozzolan content of approximately 150 kg/m³ was optimal. While the model treated pozzolan content in absolute terms, determining the optimal pozzolan-to-cement ratio can improve the overall mix design and contribute to reducing CO₂ emissions. Table 10 outlines the optimal substitution ratios of various pozzolan types, based on the collected data.

Most natural pozzolans were effective at substitution ratios between 10 and 15%, with metakaolin and scoria reaching up to 20% and pumicite allowing up to 30% substitution for normal concrete. Depending on their pozzolanic properties, industrial and agricultural byproducts could support higher substitution ratios.

Fineness, both of cement and pozzolan, was also studied, as shown in Fig. 18. The results showed that the

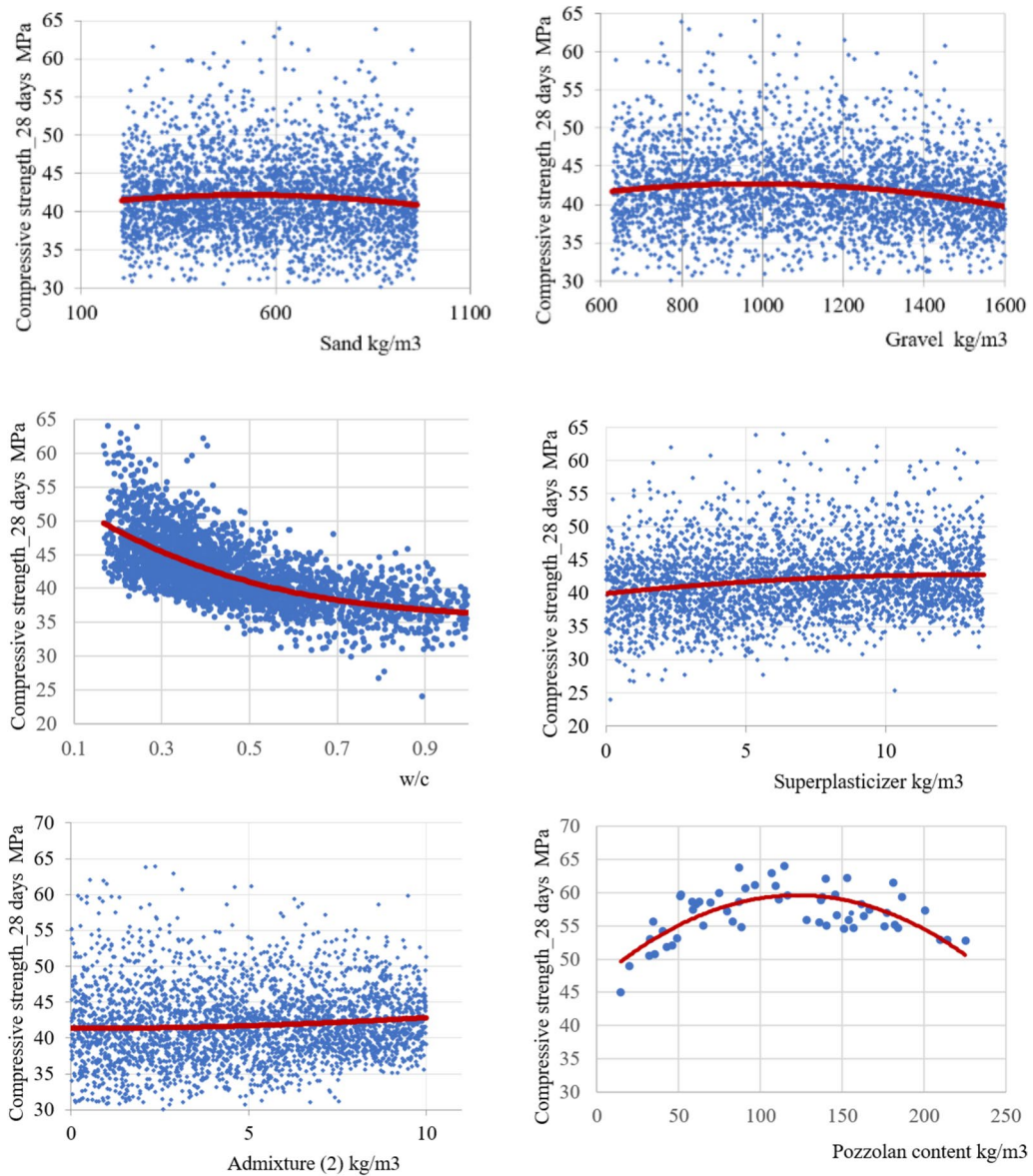


Fig. 15 Effect of component weights on compressive strength.

compressive strength of pozzolanic concrete increased as the fineness of pozzolan increased. Finer pozzolans react more readily with calcium hydroxide (Ca(OH)_2), produced during cement hydration, forming more calcium silicate hydrate (C–S–H), which is responsible for strength development. However, increased cement fineness led to a reduction in compressive strength, likely due to a larger surface area that may cause incomplete hydration. Over time, this effect may stabilize, suggesting that using finer pozzolan with coarser cement could be advantageous.

Regarding grinding methods, both inter-grinding and separate grinding had a similar effect on compressive strength, with separate grinding yielding slightly higher values. The presence of admixtures, particularly when used alongside superplasticizers, further enhanced compressive strength.

In conclusion, the synthetic data and model results highlighted the importance of optimizing cement and pozzolan content, considering local pozzolan availability, fineness of materials, and the use of admixtures to achieve the desired compressive strength while reducing resource use and emissions. The proposed model

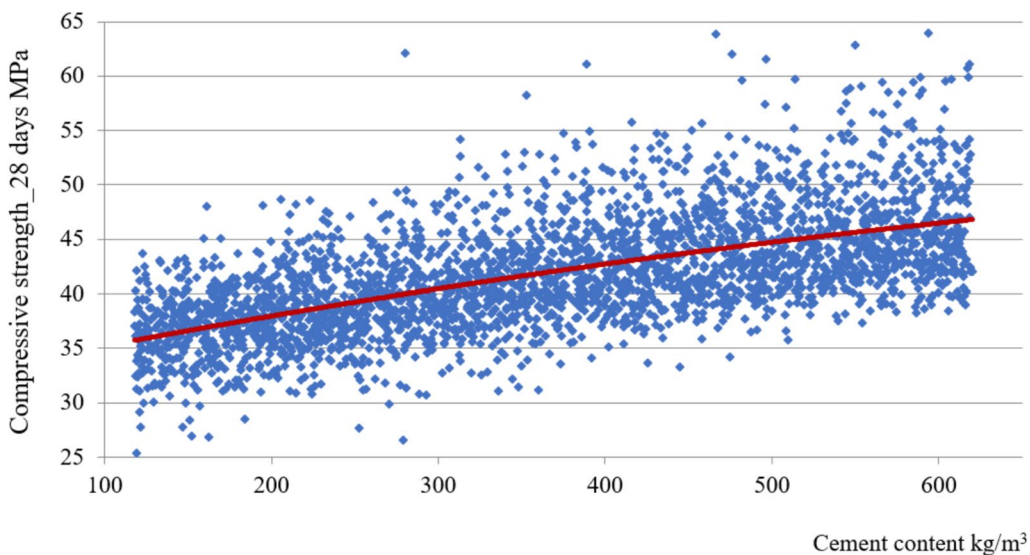


Fig. 16 Effect of cement content on compressive strength.

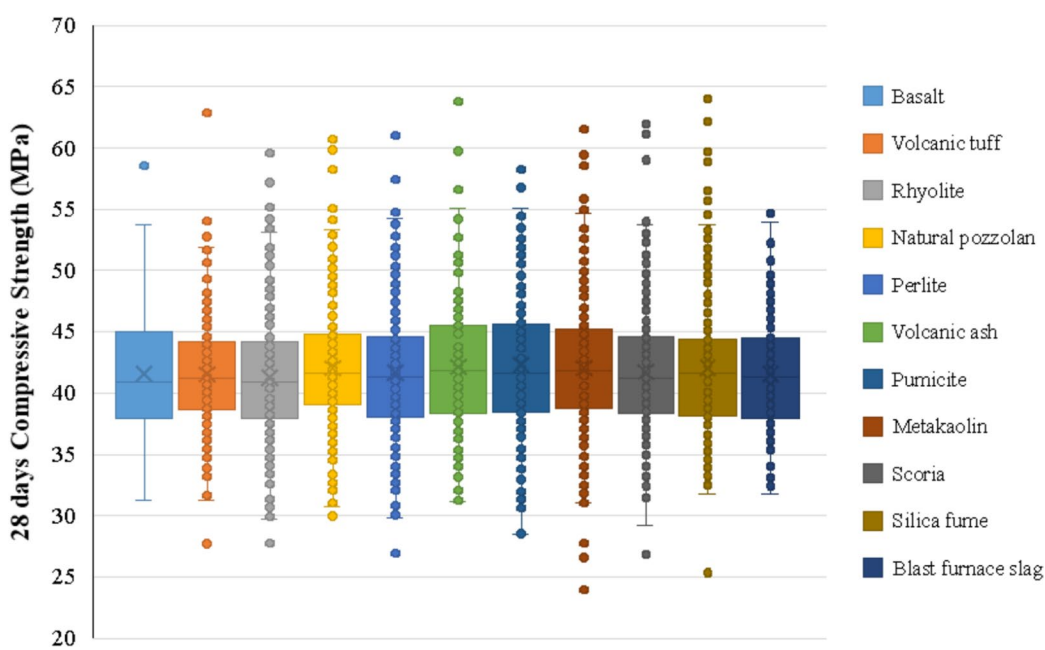


Fig. 17 Effect of pozzolan type on compressive strength.

results underscore the critical role of cement content in achieving the desired compressive strength. Optimizing the minimum cement content necessary for the specific design strength is essential. Selection of pozzolan type depends on its pozzolanic activity, availability, ease of preparation, and cost. NPz substitution typically ranges from 10 to 15%, except for metakaolin and scoria, which can reach 20%, and pumicite, which may increase to 30%. APz can achieve even higher substitution ratios.

Finer pozzolans generally lead to higher compressive strength, and it is recommended to use separate grinding for slightly better results when replacing cement with pozzolan. However, this recommendation differs from Ghiasvand et al. (2014), who advocated for inter-grinding pozzolan with clinker as a more energy-efficient technique while enhancing compressive strength.

With the aid of the VBSA, the trained model could consider the absolute effect of each parameter, which clarifies

Table 10 Optimal substitution ratios for different pozzolan types.

Type of pozzolan	Optimum substitution ratio (range)	Substitute for
Dealuminated Kaolin DK	25%	Cement
Calcined clay	20%	Cement
Metakaolin	(7.5–20)%	Cement
Scoria	20%	Cement
Trass	20–25%	Clinker/cement
Volcanic Tuffs	10%	Cement
Basalt	7.5–15%	Cement
Trachyte	Not more than 25%	Cement
Zeolite	3%	Clinker
Pumicite	20–30%	Cement
Fly ash FA	15–35%	Cement
Silica fume SF	10%	Cement
Blast furnace slag BFS	20%	Cement

the total effect of each parameter over time. Upon the VBSA results, it was noticed that the total effect of using an additional type of pozzolan was high, although its main effect was not noticeable. Then, the model's recommendations include using two types of pozzolan, incorporating admixtures, paying attention to the fineness of cement and pozzolan, and favoring separate grinding for optimal compressive strength.

Finally, the proposed framework—combining DRNNs with VBSA—is designed to assist engineers and material designers in selecting and optimizing concrete mix designs without requiring extensive lab trials. Specifically, industry professionals can use the model to predict compressive strength for various combinations of pozzolan types, proportions, admixtures, and mix ratios before physical testing. Also, the proposed framework

can be used to evaluate trade-offs between performance and sustainability (e.g., maximizing strength while minimizing cement content) and to explore optimal substitution ratios for available local pozzolans, as shown in Table 10, helping reduce costs and environmental impact. This predictive capability is especially beneficial in projects with tight timelines, budgets, or sustainability goals.

6 Conclusions

This research advances the field of sustainable concrete production by optimizing pozzolanic cement mixtures, contributing to the global effort to reduce CO₂ emissions in the cement industry. Using a hybrid framework that combines machine learning and sensitivity analysis, the study leverages both experimental and synthetic data to model concrete compressive strength with high precision. The proposed model, based on DRNNs, achieved a coefficient of determination (R^2) of 0.94 and RMSE within ± 3 MPa, confirming its accuracy in predicting compressive strength across a diverse dataset. By applying VBSA, the model quantitatively identified the most influential parameters affecting compressive strength. Cement content ranked as the most critical factor (total sensitivity index ≈ 0.65), followed by water content, pozzolan type, and admixture dosage. The model also revealed strong interaction effects—especially for secondary pozzolan types and fineness—where their total effects were substantial ($S_i^T > 0.20$) despite low direct contributions. These findings provide measurable insight into the complex behavior of pozzolanic systems.

The DRNN-VBSA framework is designed to be scalable and modular. It can be retrained using local data, deployed in user-friendly tools, and integrated into existing design workflows. The model

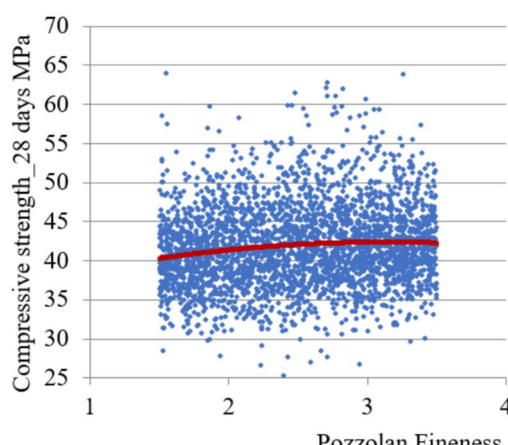
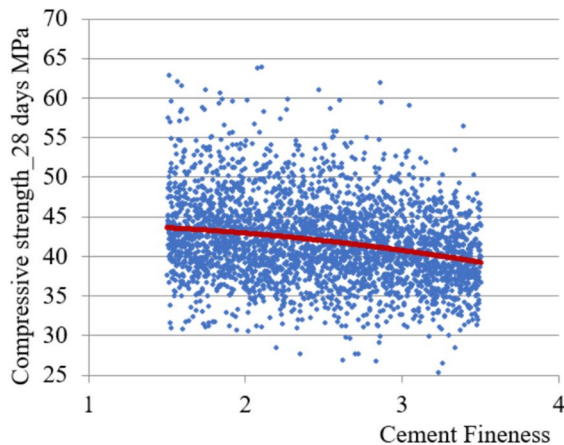


Fig. 18 Effect of fineness on compressive strength after 28 days.



demonstrated strong generalization capability with its foundation in a broad input domain, spanning 15 laboratory datasets and 3,000 augmented samples. This allows engineers to generate rapid strength predictions and optimize mix designs based on measurable targets, such as achieving 28-day strengths of ≥ 40 MPa while minimizing cement use. The study's findings are consistent with prior literature and refine it through quantitative thresholds. For example, optimal pozzolan substitution ratios were found to be 10–15% for natural pozzolans like volcanic ash, and up to 20–30% for metakaolin and pumicite. Finer pozzolans (≥ 8000 cm²/g) enhanced strength by 6–10 MPa compared to coarser ones. Superplasticizer dosages around 13 kg/m³ and cement contents ≥ 300 kg/m³ were associated with the highest compressive strength. Separate grinding marginally outperformed inter-grinding in terms of strength (+1–2 MPa), while the latter remains preferable for energy efficiency. Combinations of two pozzolan types outperformed single-pozzolan mixes, highlighting synergistic effects that were evident in the total sensitivity indices. Cement content remained the dominant driver of compressive strength across all curing stages, with other factors—such as gravel content, water-to-cement ratio, admixture use, and grinding method—becoming more influential when evaluated for their interactive contributions. Between 28 and 90 days of curing, pozzolan-related parameters (type, content, and grinding method) became increasingly significant. Synthetic data further pinpointed optimal weight ranges: 100–150 kg/m³ for pozzolan, 13 kg/m³ for superplasticizer, and water-to-cement ratios of 0.35–0.45 for high-strength applications. These ranges serve as precise benchmarks for performance-based mix optimization.

This study also opens measurable avenues for future research. Promising directions include testing hybrid natural-synthetic pozzolan blends, refining multi-admixture strategies, and expanding the framework to predict durability indicators such as sulfate resistance and chloride permeability, once reliable long-term datasets are available. Integrating life cycle assessment (LCA) tools is also recommended to evaluate environmental trade-offs in pozzolan sourcing, grinding energy, and admixture production, particularly in varying geographic contexts. The proposed DRNN-VBSA model ultimately forms a foundation for data-driven, sustainable, and high-performance concrete mix design.

Authors contributions

DMA: data curation; investigation; validation; writing—original draft. MO: formal analysis; investigation; software; validation; supervision; writing—original

draft; writing—review and editing. MFMF: conceptualization; funding acquisition; methodology; project administration; resources; supervision; writing—review and editing. RO: data curation; investigation. MKN: conceptualization; data curation; funding acquisition; methodology; project administration; resources; supervision; writing—review and editing.

Funding

Open access funding provided by The Science, Technology & Innovation Funding Authority (STDF) in cooperation with The Egyptian Knowledge Bank (EKB). This work has received funding from the project titled "Eco-friendly Pozzolanic Cement: From Research to Practical Application in Construction Industry" in the frame of the program "Applied Sciences Research". This work was supported by the Science, Technology, and Innovation Funding Authority (STDF) under the grant agreement number (47438).

Data availability

The datasets generated and/or analyzed in the present study are available upon a reasonable request.

Declarations

Ethics approval and consent to participate

Not applicable.

Consent for publication

Not applicable.

Competing interests

The authors declare that they have no known competing financial interests or personal relationships that could have appeared to influence the work reported in this paper.

Received: 20 January 2025 Accepted: 26 June 2025

Published online: 03 September 2025

References

- Abrão, P. C. R. A., Cardoso, F. A., & John, V. M. (2020). Efficiency of Portland-pozzolana cements: Water demand, chemical reactivity and environmental impact. *Construction and Building Materials*, 247, 118546. <https://doi.org/10.1016/j.conbuildmat.2020.118546>
- Al-Chaar, G. (2013). Natural pozzolan as a partial substitute for cement in concrete. *The Open Construction and Building Technology Journal*, 7, 33–42. <https://doi.org/10.2174/1874836801307010033>
- Al-Hashem, M. N., et al. (2022). Mechanical and durability evaluation of metakaolin as cement replacement material in concrete (in Eng). *Materials (Basel)*. <https://doi.org/10.3390/ma15227868>
- Ali, A. A. M., Negm, A. M., Bady, M. F., Ibrahim, M. G. E., & Suzuki, M. (2016). Environmental impact assessment of the Egyptian cement industry based on a life-cycle assessment approach: a comparative study between Egyptian and Swiss plants. *Clean Technologies and Environmental Policy*, 18(4), 1053–1068. <https://doi.org/10.1007/s10098-016-1096-0>
- Almutairi, A., & Owais, M. (2024). Active traffic sensor location problem for the uniqueness of path flow identification in large-scale networks. *IEEE Access*.
- Almutairi, A., & Owais, M. (2025). Reliable vehicle routing problem using traffic sensors augmented information. *Sensors*, 25(7), 2262.
- Almutairi, A., Owais, M., & Ahmed, A. S. (2024). Notes on bus user assignment problem using section network representation method. *Applied Sciences*, 14(8), 3406.
- Alpaydin, E. (2020). *Introduction to machine learning*. MIT press.
- Alshehri, A., Owais, M., Gyani, J., Aljarbou, M. H., & Alsulamy, S. (2023). Residual neural networks for origin–destination trip matrix estimation from traffic sensor information. *Sustainability*, 15(13), 9881.
- Altwair, N. M., & Kabir, S (2010). Green concrete structures by replacing cement with pozzolanic materials to reduce greenhouse gas emissions for sustainable environment. In: 6th International Engineering and Construction Conference, Cairo, Egypt, vol. 17, pp. 1126–1130

Ashrafiyan, A., Behnood, A., Golafshani, E. M., Panahi, E., & Berenjian, J. (2024a). Toward presenting an ensemble meta-model for evaluation of pozzolanic mixtures incorporating industrial by-products. *Structural Concrete*, 25(2), 1305–1323. <https://doi.org/10.1002/suco.202300452>

Ashrafiyan, A., Behnood, A., Golafshani, E. M., Panahi, E., & Berenjian, J. (2024b). Toward presenting an ensemble meta-model for evaluation of pozzolanic mixtures incorporating industrial by-products. *Structural Concrete*, 25(2), 1305–1323.

Avci, O., Abdeljaber, O., Kiranyaz, S., Hussein, M., Gabbouj, M., & Inman, D. J. (2021). A review of vibration-based damage detection in civil structures: From traditional methods to Machine Learning and Deep Learning applications. *Mechanical Systems and Signal Processing*, 147, Article 107077.

Ayene, H., Geremew, A., & Amenu, T. (2023). Potential use of scoria as a cementitious material for green concrete production. *Advances in Civil Engineering*, 2023(1), 5532027.

Belaïd, F. (2022). How does concrete and cement industry transformation contribute to mitigating climate change challenges? *Resources, Conservation & Recycling Advances*, 15, 200084. <https://doi.org/10.1016/j.jrcradv.2022.200084>

Bishop, C. M. (2006). *Pattern recognition and machine learning*. Springer.

Chihaoui, R., Siad, H., Senhadji, Y., Mouli, M., Nefoussi, A. M., & Lachemi, M. (2022). Efficiency of natural pozzolan and natural perlite in controlling the alkali-silica reaction of cementitious materials. *Case Studies in Construction Materials*, 17, Article e01246.

Chindaprasirt, P., & Rukzon, S. (2008). Strength, porosity and corrosion resistance of ternary blend Portland cement, rice husk ash and fly ash mortar. *Construction and Building Materials*, 22(8), 1601–1606.

Deboucha, W., Oudjit, M. N., Bouzid, A., & Belagraa, L. (2015). Effect of incorporating blast furnace slag and natural pozzolana on compressive strength and capillary water absorption of concrete. *Procedia Engineering*, 108, 254–261. <https://doi.org/10.1016/j.proeng.2015.06.145>

Dembovska, L., Bajare, D., Pundiene, I., & Vitola, L. (2017). Effect of pozzolanic additives on the strength development of high performance concrete. *Procedia Engineering*, 172, 202–210.

Dietterich, T. G. (2000). Ensemble methods in machine learning. *International workshop on multiple classifier systems* (pp. 1–15). Springer.

Du, H., Gao, H. J., & DaiPang, S. (2016). Improvement in concrete resistance against water and chloride ingress by adding graphene nanoplatelet. *Cement and Concrete Research*, 83, 114–123.

Dunuweera, S., & Rajapakse, R. (2018). Cement types, composition, uses and advantages of nanocement, environmental impact on cement production, and possible solutions. *Advances in Materials Science and Engineering*, 2018(1), 4158682.

Dwivedi, V., Singh, N., Das, S., & Singh, N. (2006). A new pozzolanic material for cement industry: Bamboo leaf ash. *International Journal of Physical Sciences*, 1(3), 106–111.

Eldahroty, K. E. H., Farghali, A. A., Shehata, N., & Mohamed, O. A. (2023). Valorification of Egyptian volcanic tuff as eco-sustainable blended cementitious materials. *Scientific Reports*, 13(1), 3653. <https://doi.org/10.1038/s41598-023-30612-0>

El-Didamony, H., Helmy, I., Osman, R. M., & Habboud, A. (2015). Basalt as pozzolana and filler in ordinary Portland cement. *American Journal of Engineering and Applied Sciences*, 8(2), 263.

Fodil, D., & Mohamed, M. (2018). Compressive strength and corrosion evaluation of concretes containing pozzolana and perlite immersed in aggressive environments. *Construction and Building Materials*, 179, 25–34. <https://doi.org/10.1016/j.conbuildmat.2018.05.190>

Ghiasvand, E., Ramezanianpour, A. A., & Ramezanianpour, A. M. (2014). Effect of grinding method and particle size distribution on the properties of Portland-pozzolan cement. *Construction and Building Materials*, 53, 547–554. <https://doi.org/10.1016/j.conbuildmat.2013.11.072>

Golewski, G. L. (2022). The role of pozzolanic activity of siliceous fly ash in the formation of the structure of sustainable cementitious composites. *Sustainable Chemistry*, 3(4), 520–534.

Goodfellow, I., Bengio, Y., & Courville, A. (2016). *Deep learning (adaptive computation and machine learning series)*. MIT Press.

Haenlein, M., & Kaplan, A. (2019). A brief history of artificial intelligence: On the past, present, and future of artificial intelligence. *California Management Review*, 61(4), 5–14.

Hamada, H. M., Abed, F., Beddu, S., Humada, A. M., & Majdi, A. (2023). Effect of Volcanic Ash and Natural Pozzolana on mechanical properties of sustainable cement concrete: A comprehensive review. *Case Studies in Construction Materials*, 19, e02425. <https://doi.org/10.1016/j.cscm.2023.e02425>

Hammat, S., Menadi, B., Kenai, S., Thomas, C., Kirgiz, M. S., & Sousa Galdino, A. G. D. (2021). The effect of content and fineness of natural pozzolana on the rheological, mechanical, and durability properties of self-compacting mortar. *Journal of Building Engineering*, 44, 103276. <https://doi.org/10.1016/j.jobe.2021.103276>

Haq, I., et al. (2024). Synergistic effect of fly ash and stone dust on foam concrete under saline environment: Mechanical, non-destructive and machine learning approaches. *Advances in Concrete Construction*, 18(4), 237.

Hassan, E. M., Abdul-Wahab, S. A., Abdo, J., & Yetilmezsoy, K. (2019). Production of environmentally friendly cements using synthetic zeolite catalyst as the pozzolanic material. *Clean Technologies and Environmental Policy*, 21(9), 1829–1839. <https://doi.org/10.1007/s10098-019-01752-7>

Hassanein, Y. A.-A., Farghal, O. A., Raheem, S. A., Fahmy, M., & Nafadi, M. (2022). Results of a research study on six types of cements, A technical report submitted by Assuit University to CEMEX.

He, K., Zhang, S., Ren, S., & Sun, J. (2015). Delving deep into rectifiers: Surpassing human-level performance on imagenet classification. In: *Proceedings of the IEEE international conference on computer vision*, pp. 1026–1034.

Hung, C.-C., Su, Y.-F., & Su, Y.-M. (2018). Mechanical properties and self-healing evaluation of strain-hardening cementitious composites with high volumes of hybrid pozzolan materials. *Composites Part b: Engineering*, 133, 15–25.

Hussain, Z., & Akbar, A. (2022). Diagnostics through residual plots in binomial regression addressing chemical species data. *Mathematical Problems in Engineering*, 2022, 4375945.

Idriss, L. K., & Owais, M. (2024). Global sensitivity analysis for seismic performance of shear wall with high-strength steel bars and recycled aggregate concrete. *Construction and Building Materials*, 411, Article 134498.

Ioffe, S., & Szegedy, C. (2015). Batch normalization: Accelerating deep network training by reducing internal covariate shift. *arXiv preprint arXiv:1502.03167*.

Ivanovic, M., & Radovanovic, M. (2015). Modern machine learning techniques and their applications. In: *International conference on electronics, communications and networks*.

Jiang, L., Xie, Y., Wen, X., & Ren, T. (2020). Modeling highly imbalanced crash severity data by ensemble methods and global sensitivity analysis. *Journal of Transportation Safety & Security*, pp. 1–23.

Jokar, Z., & Mokhtar, A. (2018). Policy making in the cement industry for CO₂ mitigation on the pathway of sustainable development- A system dynamics approach. *Journal of Cleaner Production*, 201, 142–155. <https://doi.org/10.1016/j.jclepro.2018.07.286>

Joshua, O., Matawal, D. S., Akinwumi, T. D., Olusola, K. O., Ogurro, A. S., & Lawal, R. B. (2018). Development of a fully pozzolanic binder for sustainable construction: Whole cement replacement in concrete applications. *International Journal of Civil Engineering and Technology*, 9(2), 1–2.

Juenger, M. C. G., & Siddique, R. (2015). Recent advances in understanding the role of supplementary cementitious materials in concrete. *Cement and Concrete Research*, 78, 71–80. <https://doi.org/10.1016/j.cemconres.2015.03.018>

Kao, C.-Y., Shen, C.-H., Jan, J.-C., & Hung, S.-L. (2018). A computer-aided approach to pozzolanic concrete mix design. *Advances in Civil Engineering*, 2018(1), 4398017.

Karim, R., Islam, M. H., Datta, S. D., & Kashem, A. (2024). Synergistic effects of supplementary cementitious materials and compressive strength prediction of concrete using machine learning algorithms with SHAP and PDP analyses. *Case Studies in Construction Materials*, 20, Article e02828.

Katare, V. D., & Madurwar, M. V. (2020). Design and investigation of sustainable pozzolanic material. *Journal of Cleaner Production*, 242, 118431. <https://doi.org/10.1016/j.jclepro.2019.118431>

Koneru, V. S., Kolli, S. N. C., Vemuri, V. G., Gurrappa, K., Ghorpade, V. G., & Hanchate, S. R. (2023). Development of optimum sustainable metakaolin replaced cement concrete based on homogeneity, compressive strength and rapid chloride ion penetration. *Materials Today: Proceedings*, 80, 1306–1310.

Langley, P. (2011). The changing science of machine learning. *Machine Learning*, 82(3), 275–279.

Marani, A., & Nehdi, M. L. (2020). Machine learning prediction of compressive strength for phase change materials integrated cementitious composites. *Construction and Building Materials*, 265, Article 120286.

McCarthy, M. J., & Dyer, T. D. (2019). Pozzolanas and pozzolanic materials. *Lea's Chemistry of Cement and Concrete*, 5, 363–467.

Moawad, M., Ragab, A., & Younis, S. (2023). Effect of the natural pozzolanic basalt on high strength concrete. *Mansoura Engineering Journal*. <https://doi.org/10.58491/2735-4202.3063>

Moawad, M. S., Younis, S., & Ragab, A. E. L. R. (2021). Assessment of the optimal level of basalt pozzolana blended cement replacement against concrete performance. *Journal of Engineering and Applied Science*, 68(1), 42. <https://doi.org/10.1186/s44147-021-00046-4>

Moradi, M., Khaleghi, M., Salimi, J., Farhangi, V., & Ramezanianpour, A. (2021). Predicting the compressive strength of concrete containing metakaolin with different properties using ANN. *Measurement*, 183, Article 109790.

Morris, M. D. (1991). Factorial sampling plans for preliminary computational experiments. *Technometrics*, 33(2), 161–174.

Mottakin, M., Datta, S. D., Hossain, M. M., Sobuz, M. H. R., Rahman, S. A., & Alhartai, M. (2024). Evaluation of textile effluent treatment plant sludge as supplementary cementitious material in concrete using experimental and machine learning approaches. *Journal of Building Engineering*, 96, Article 110627.

Mousavinezhad, S., Garcia, J. M., Toledo, W. K., & Newton, C. M. (2023). A locally available natural pozzolan as a supplementary cementitious material in Portland cement concrete. *Buildings*, 13(9), 2364.

Müller, A. C., & Guido, S. (2016). *Introduction to machine learning with Python: A guide for data scientists*. O'Reilly Media Inc.

Narmatha, M., & Felixkala, T. (2016). Meta kaolin—the best material for replacement of cement in concrete. *IOSR Journal of Mechanical and Civil Engineering*, 13(4), 66–71.

Nayaka, R. R., Alengaram, U. J., Jumaat, M. Z., Yusoff, S. B., & Alnahhal, M. F. (2018). High volume cement replacement by environmental friendly industrial by-product palm oil clinker powder in cement–lime masonry mortar. *Journal of Cleaner Production*, 190, 272–284.

Nguyen, T. G., & de Kok, J.-L. (2007). Systematic testing of an integrated systems model for coastal zone management using sensitivity and uncertainty analyses. *Environmental Modelling & Software*, 22(11), 1572–1587.

Nossent, J., Elsen, P., & Bauwens, W. (2011). Sobol' sensitivity analysis of a complex environmental model. *Environmental Modelling & Software*, 26(12), 1515–1525.

Nourredine, G., Kerdal, D. E., Nouria, K., & Rachida, I. (2021). Potential use of activated Algerian natural pozzolan powder as a cement replacement material. *European Journal of Environmental and Civil Engineering*, 25(6), 967–987.

Omrale, M., & Rabehi, M. (2020). Effect of natural pozzolan and recycled concrete aggregates on thermal and physico-mechanical characteristics of self-compacting concrete. *Construction and Building Materials*, 247, Article 118576. <https://doi.org/10.1016/j.conbuildmat.2020.118576>

Owais, M. (2024). How to incorporate machine learning and microsimulation tools in travel demand forecasting in multi-modal networks. *Expert Systems with Applications* 125563.

Owais, M. (2024a). Deep learning for integrated origin–destination estimation and traffic sensor location problems. *IEEE Transactions on Intelligent Transportation Systems*, 25(7), 6501–6513.

Owais, M. (2024c). Preprocessing and postprocessing analysis for hot-mix asphalt dynamic modulus experimental data. *Construction and Building Materials*, 450, Article 138693.

Owais, M., & Ahmed, A. S. (2022). Frequency based transit assignment models: Graph formulation study. *IEEE Access*, 10, 62991–63003.

Owais, M., Ahmed, A. S., Moussa, G. S., & Khalil, A. A. (2020a). An optimal metro design for transit networks in existing square cities based on non-demand criterion. *Sustainability*, 12(22), 9566.

Owais, M., Ahmed, A. S., Moussa, G. S., & Khalil, A. A. (2021). Integrating underground line design with existing public transportation systems to increase transit network connectivity: Case study in greater Cairo. *Expert Systems with Applications*, 167, Article 114183.

Owais, M., & Alshehri, A. (2020). Pareto optimal path generation algorithm in stochastic transportation networks. *IEEE Access*, 8, 58970–58981.

Owais, M., Alshehri, A., Gyani, J., Aljarbou, M. H., & Alsulamy, S. (2024). Prioritizing rear-end crash explanatory factors for injury severity level using deep learning and global sensitivity analysis. *Expert Systems with Applications*, 245, Article 123114.

Owais, M., & El Sayed, M. A. (2025). Red light crossing violations modelling using deep learning and variance-based sensitivity analysis. *Expert Systems with Applications*, 267, Article 126258.

Owais, M., & Idriss, L. K. (2024). Modeling green recycled aggregate concrete using machine learning and variance-based sensitivity analysis. *Construction and Building Materials*, 440, Article 137393.

Owais, M., & Matouk, A. E. (2021). A factorization scheme for observability analysis in transportation networks. *Expert Systems with Applications*, 174, Article 114727.

Owais, M., & Moussa, G. S. (2024). Global sensitivity analysis for studying hot-mix asphalt dynamic modulus parameters. *Construction and Building Materials*, 413, Article 134775.

Owais, M., Moussa, G., Abbas, Y., & El-Shabrawy, M. (2013). Optimal frequency setting for circular bus routes in Urban Areas. *JES. Journal of Engineering Sciences*, 41(5), 1796–1811.

Owais, M., Moussa, G. S., & Hussain, K. F. (2019). Sensor location model for O/D estimation: Multi-criteria meta-heuristics approach. *Operations Research Perspectives*, 6, Article 100100.

Owais, M., Moussa, G. S., & Hussain, K. F. (2020b). Robust deep learning architecture for traffic flow estimation from a subset of link sensors. *Journal of Transportation Engineering, Part a: Systems*, 146(1), 04019055.

Ozvan, A., Tapan, M., Erik, O., Efe, T., & Depci, T. (2012). Compressive strength of scoria added Portland cement concretes. *Gazi University Journal of Science*, 25(3), 769–775.

Paiva, H., Velosa, A., Cachim, P., & Ferreira, V. (2012). Effect of metakaolin dispersion on the fresh and hardened state properties of concrete. *Cement and Concrete Research*, 42(4), 607–612.

Papadakis, V. G. (2000). Effect of supplementary cementing materials on concrete resistance against carbonation and chloride ingress. *Cement and Concrete Research*, 30(2), 291–299.

Pellinen, T.K. (2002). Investigation of the use of dynamic modulus as an indicator of hot-mix asphalt performance.

Pianosi, F., et al. (2016). Sensitivity analysis of environmental models: A systematic review with practical workflow. *Environmental Modelling & Software*, 79, 214–232.

Ramachandran, P., Zoph, B., & Le, Q. V. (2017). Searching for activation functions. *arXiv preprint arXiv:1710.05941*.

Ramezanianpour, A. A. (2014). Cement replacement materials. *Springer Geochemistry/mineralogy*, DOI, 10, 978–983.

Rashwan, M. A., El Saeed, R. L., & Hegazy, A. A. (2023a). Tracking the pozzolanic activity of mafic rock powder on durability performance of cement pastes under adverse conditions: Physico-mechanical properties, mineralogy, microstructure, and heat of hydration. *Journal of Building Engineering*, 71, Article 106485.

Rashwan, M. A., Lasheen, E. S. R., & Hegazy, A. A. (2023b). Tracking the pozzolanic activity of mafic rock powder on durability performance of cement pastes under adverse conditions: Physico-mechanical properties, mineralogy, microstructure, and heat of hydration. *Journal of Building Engineering*, 71, 106485. <https://doi.org/10.1016/j.jobe.2023.106485>

Rebouh, R., Boukhatem, B., Ghrici, M., & Taghit-Hamou, A. (2017). A practical hybrid NNGA system for predicting the compressive strength of concrete containing natural pozzolan using an evolutionary structure. *Construction and Building Materials*, 149, 778–789. <https://doi.org/10.1016/j.conbuildmat.2017.05.165>

Rosenthal, C. (2003). Certifying knowledge: The sociology of a logical theorem in artificial intelligence. *American Sociological Review*, 68(4), 623–644.

Saisana, M., Saltelli, A., & Tarantola, S. (2005). Uncertainty and sensitivity analysis techniques as tools for the quality assessment of composite indicators. *Journal of the Royal Statistical Society: Series A (Statistics in Society)*, 168(2), 307–323.

Salami, B. A., Olayiwola, T., Oyehan, T. A., & Raji, I. A. (2021). Data-driven model for ternary-blend concrete compressive strength prediction using machine learning approach. *Construction and Building Materials*, 301, Article 124152.

Saltelli, A., et al. (2008). *Global sensitivity analysis: the primer*. Wiley.

Saltelli, A., Ratto, M., Tarantola, S., Campolongo, F., & Commission, E. (2006). Sensitivity analysis practices: Strategies for model-based inference. *Reliability Engineering & System Safety*, 91(10–11), 1109–1125.

Schmidhuber, J. (2015). Deep learning in neural networks: An overview. *Neural Networks*, 61, 85–117.

Schwartz, C. W., Li, R., Ceylan, H., Kim, S., & Gopalakrishnan, K. (2013). Global sensitivity analysis of mechanistic–empirical performance predictions for flexible pavements. *Transportation Research Record*, 2368(1), 12–23.

Senhadji, Y., Escadeillas, G., Khelafi, H., Mouli, M., & Benosman, A. S. (2012). Evaluation of natural pozzolan for use as supplementary cementitious material. *European Journal of Environmental and Civil Engineering*, 16(1), 77–96.

Shin, M.-J., Guillaume, J. H., Croke, B. F., & Jakeman, A. J. (2013). Addressing ten questions about conceptual rainfall–runoff models with global sensitivity analyses in R. *Journal of Hydrology*, 503, 135–152.

Sieber, A., & Uhlenbrook, S. (2005). Sensitivity analyses of a distributed catchment model to verify the model structure. *Journal of Hydrology*, 310(1–4), 216–235.

Spear, R., & Hornberger, G. (1980). Eutrophication in peat inlet—II. Identification of critical uncertainties via generalized sensitivity analysis. *Water Research*, 14(1), 43–49.

Szegedy, C., et al. (2015). Going deeper with convolutions. In: *Proceedings of the IEEE conference on computer vision and pattern recognition*, pp. 1–9.

Taffese, W. Z., & Sistonen, E. (2017). Machine learning for durability and service-life assessment of reinforced concrete structures: Recent advances and future directions. *Automation in Construction*, 77, 1–14.

Taffese, W. Z., Sistonen, E., & Puttonen, J. (2015). CaPrM: Carbonation prediction model for reinforced concrete using machine learning methods. *Construction and Building Materials*, 100, 70–82.

Tarantola, S., Becker, W., & Zeitz, D. (2012). A comparison of two sampling methods for global sensitivity analysis. *Computer Physics Communications*, 183(5), 1061–1072.

Tsai, C.-L., Cai, Z., & Wu, X. (1998). The examination of residual plots. *Statistica Sinica*, pp. 445–465.

Waghmare, J. D., Patil, S. S., Patil, S. M., & Maske, M. (2021). Study and review of properties and applications of Portland Pozzolana cement. *ASEAN Journal of Science and Engineering*, 1(1), 13–18.

William, C., Akobo, I., & Ngekpe, B. (2019). Effect of metakaolin as a partial replacement for cement on the compressive strength of high strength concrete at varying water/binder ratios. *International Journal of Civil Engineering*, 6, 1–6. <https://doi.org/10.14445/23488352/IJCE-V6I1P101>

Záleská, M., et al. (2018). Physical and chemical characterization of technogenic pozzolans for the application in blended cements. *Construction and Building Materials*, 160, 106–116.

Zang, J., Wang, L., Liu, Z., Zhang, Q., Hua, G., spsampsps Zheng, N. (2018). Attention-based temporal weighted convolutional neural network for action recognition. In: *IFIP international conference on artificial intelligence applications and innovations*. Springer, pp. 97–108.

Zeyad, A. M., & Almalki, A. (2021). Role of particle size of natural pozzolanic materials of volcanic pumice: flow properties, strength, and permeability. *Arabian Journal of Geosciences*, 14(2), 107. <https://doi.org/10.1007/s12517-020-06443-y>

Publisher's Note

Springer Nature remains neutral with regard to jurisdictional claims in published maps and institutional affiliations.

Dina M. Abdelsattar candidate at Civil Engineering Department, Faculty of Engineering, Assiut University, Egypt.

Mahmoud Owais received an M.S. in transportation planning and a Ph.D. in transit planning from the University of Assiut in 2011 and 2014, respectively. He is currently a professor of transportation planning and traffic engineering with the Civil Engineering Department, Faculty of Engineering, Assiut University. He has published more than 40 studies with over 1,300 citations and completed more than 700 reviews in well-reputed journals such as; IEEE Transactions On ITS, Expert Systems with Applications, and Accident Analysis &

Prevention. He also serves as Associate Editor for the journal Innovative Infrastructure Solutions in Springer. For more information, visit the link: <https://scholar.google.com.eg/citations?user=UNwlx2MAAAAJ&hl=enM>.

Mohamed F. M. Fahmy received his Ph.D. in Structural Engineering from Ibaraki University, Japan, in 2010. From 2014 to 2020, he worked as an Associate Professor at Southeast University, China, where his research focused on structural strengthening/repair and innovation using fiber-reinforced polymers. He has authored over 100 peer-reviewed research papers, including more than 60 indexed in SCI journals, co-authored seven internationally published books, and holds four registered patents. His areas of expertise include damage control, structural strengthening, seismic-resistant systems, prefabricated construction systems, and sustainable engineering practices.

Rahma Osman is a researcher at Civil Engineering Department, Faculty of Engineering, Assiut University, Egypt.

Mohamed K. Nafadi is an Assistant Professor of Structural Engineering at Civil Engineering Department, Faculty of Engineering, Assiut University. He earned his B.Sc. from Assiut University and both his M. Sc. and Ph.D. from North Carolina State University (NCSU) in USA. He is a Fulbright Fellow and a recipient of the Martin P. Korn Award from the Precast/Prestressed Concrete Institute (PCI). His areas of expertise include precast and prestressed concrete structures, material properties and strength, and finite element modeling of structural components and systems.